Model-Free Backward and Forward Nonlinear PDEs for Implied Volatility

PETER CARR, ANDREY ITKIN, AND SASHA STOIKOV

AQ1 **PETER CARR**
is chair of the finance and risk engineering department and a professor in the Tandon School of Engineering at New York University in Brooklyn, NY.
petercarr@nyu.edu

ANDREY ITKIN
is an adjunct professor in finance and risk engineering in the Tandon School of Engineering at New York University in Brooklyn, NY.
aitkin@nyu.edu

SASHA STOIKOV
is a senior research associate in the School of Operations Research and Information Engineering at Cornell University in New York, New York.
sfs33@cornell.edu

KEY FINDINGS

- In this article, we derive backward and forward quasilinear parabolic PDEs that govern the implied volatility of a contingent claim whenever the latter is well-defined. Alternatively, we have derived a forward nonlinear hyperbolic PDE of the first order, which also governs evolution of the implied volatility in (K, T, Z) space. We discuss suitable initial and boundary conditions for those PDEs.
- We develop an iterative numerical method to solve the PDEs by using a finite-difference approach. The method is of second order of approximation in both space and time, is unconditionally stable, and preserves positivity of the solution.
- Using this method, we compute the PDE implied volatility and find that our intuition behind the main idea of the article is correct. In other words, performance of the finite-difference solver exceeds that of the traditional approach by factor of forty. However, this result is subject to some details, which are highlighted in the article.

ABSTRACT: *The authors derive backward and forward nonlinear PDEs that govern the implied volatility of a contingent claim whenever the latter is well-defined. This would include at least any contingent claim written on a positive stock price whose payoff at a possibly random time is convex. The authors also discuss suitable initial and boundary conditions for those PDEs. Finally, we demonstrate how to solve them numerically by using an iterative finite-difference approach.*

TOPICS: ***Volatility measures, options****

*All articles are now categorized by topics and subtopics. **View at PM-Research.com.**

Given an option contract written on some stock, for example, the implied volatility is derived from the option price and shows what the market implies about the underlying stock volatility in the future. For instance, the implied volatility is one of six inputs used in a simple option pricing (Black-Scholes) model, but is the only one that is not directly observable in the market. The standard way to determine it by knowing the market price of the contract and the other five parameters, is to solve for the implied volatility by equating the model and market prices of the option contract.

Various reasons exists to explain why traders prefer to consider option positions in terms of the implied volatility, rather than the option price itself, see e.g., Natenberg (1994). However, in this article, our goal is not to discuss the importance of this concept. Instead, we focus on the way in which the

implied volatility is computed and the performance of this process.

The traditional method of computing the Black-Scholes implied volatility is relatively simple, see the PDE for the BS formula in Equation (1). One might say that the main problem with such an approach emerges if one needs to simultaneously compute the implied volatility for a wide set of the model (contract) parameters. Then, the iterative root solver can converge slowly because i) there is no a universal good initial guess to kick off the iterations, and ii) for some regions of the model parameters, the solution either doesn't exist at all, or is hard to find, as the sensitivity of the model price to changes in the implied volatility is very low.

Therefore, a surprising and useful idea would be to replace the algebraic equation Equation (2), which is used to determine the implied volatility, with another object, a partial differential equation (PDE), for instance. Here the surprise means that the PDE is a more complicated object than the algebraic equation, and solving the PDE (especially a nonlinear PDE) requires some special methods, usually much more complicated than a simple root solver. However, in contrast to the algebraic equation that should be solved independently at every given point e.g., in the space of option strikes and maturities, the PDE approach allows for finding the solution simultaneously in many such points by using a series of marching sweeps in time. Also, solving a linear PDE doesn't require iterations, and hence, there is no need for a good initial guess.

In this article, we demonstrate how such a PDE could be derived simply by using a general definition of the implied volatility. Moreover, we extend this idea by deriving several types of these PDEs. For instance, we obtain quasilinear backward and forward parabolic PDEs, and also nonlinear hyperbolic PDEs of the first order. As these PDEs are new and have not yet been investigated in the literature, we need to discuss suitable initial and boundary conditions that provide for the solution of these PDE to exist and be unique. We also develop an iterative numerical method to solve the PDEs by using a finite-difference approach. The method is of second order approximation in both space and time, is unconditionally stable, and preserves the positivity of the solution. Using this method, we compute the PDE-implied volatility and find that our intuition behind the main idea of the article is correct. In other words, the performance of the finite-difference solver exceeds that of the traditional approach by factor of forty. However, this result is subject to some details, which are highlighted in the last section.

Despite the fact that, in this article, the PDE approach is considered as an alternative to the traditional method of getting the implied volatility by using the root solver, the latter method has been significantly improved within the past few years. First, in Jackel (2015), modified Newton iterations were proposed to solve Equation (2). In this approach, the entire input domain is decomposed into four areas. Rational approximations are used to provide initial guesses and reduce the number of iterations. In addition, this method provides an accuracy close to machine precision. However, it breaks possible vectorization, although we don't consider that topic in this article).

In Glau et al. (2018), Jackel's approach (2015) is improved by using a bivariate Chebyshev interpolation of the implied volatility. This algorithm allows for vectorization and consists of two steps. At the offline phase, the polynomial weights of a low-rank Chebyshev interpolation of the implied volatility surface are computed and stored for four different input domains, using Jackel's algorithm (2015). This step is only performed once. During the online phase, the input data is split into four domains, and the Chebyshev interpolation is applied to each domain by choosing the precomputed nodes from the offline step.

From this perspective, the problem can also be solved by building an artificial neural network (ANN) and training it on a given data set, which will include all parameters of the contract (the spot price, the time to maturity, the strike, option price, etc.) and output the Black-Scholes implied volatility. The method of Jackel (2015) can be used when training this ANN as the golden "pricer." As such, the approach proposed in this article becomes less important; since the ANN training could be done offline, the performance of the "pricer" is less important than the accuracy. This is completely opposite to the proposed PDE approach. However, using the ANN still requires solving various problems, such as no-arbitrage, the existence of derivatives, and so forth, see Itkin (2019). In addition, the advantage of using the ANN approach, as opposed to traditional methods, is, perhaps, a property inherent to many financial models, and not only to the model we consider here.

Aside from practical importance, the existence of the model-free quasilinear parabolic PDE (or the other hyperbolic PDE) in governing the implied volatility is

an interesting fact that has not been discovered in the literature. Therefore, the novelty of this article consists in the derived equations together with the proposed numerical method of their solution.

The rest of the article is organized as follows. In the next section, we derive a backward quasilinear PDE for the implied volatility. We then use a similar approach to derive an analogous forward PDE. After that, we discuss how one can set the appropriate initial and boundary conditions for these PDEs and we derive some other PDEs for the implied volatility that have a different type (nonlinear hyperbolic rather than quasilinear parabolic equations). Following that discussion, we provide a short historical overview of splitting methods, with the ultimate goal of revealing a bridge between physics and computational fluid dynamics (CFD), where these methods were first introduced, and the modern computational finance. This is done because splitting is one of the two basic methods used to solve the derived PDEs numerically. The constructed numerical method is then described in detail, and in two Appendices. After that, the results of our numerical experiments are presented, with a comparison of two methods: i) the traditional method of finding the implied volatility by using a root solver with the Black-Scholes equation, and ii) the proposed method of solving the derived PDEs numerically, In the final section, we discuss the results obtained and conclude.

BACKWARD PDE

Consider a class of contingent claims that have a single payoff and are written on the spot price path of a single underlying risky asset. The Black-Scholes implied volatility (Hull 1997) can be defined for any such contingent claim, as long as the claim's value in the Black-Scholes model is monotonic in the volatility of the underlying asset. Standard examples include European options and American options that are optimally held alive. If the claim's value is decreasing in volatility, then the value of a short position in that claim is increasing in volatility. Hence, there is no loss in generality if implied volatility is only defined for short or long positions in claims whose value increases with volatility. We refer to any such claim as an option. This section derives a new nonlinear partial differential equation (PDE) that relates the Black-Scholes implied volatility to the option price, to the underlying stock price, and to calendar time.

The Black-Scholes implied volatility is a useful measure, as it is a market practice where, instead of quoting the option premium in the relevant currency, the options are quoted in terms of the Black-Scholes implied volatility. Over the years, option traders have developed an intuition for this quantity. However, it can be further generalized by using a similar concept, but replacing the Black-Scholes framework with another one. For instance, in Corcuera et al. (2009), this is done under a Lévy framework, and, therefore, is based on distributions that match historical returns more closely. In this article, we don't consider these generalizations, and are concentrating only on the Black-Scholes implied volatility.

Consider a fixed time horizon $t \in [0, T]$, where $T > 0$ is the time to maturity. We assume that the underlying stock price S is strictly positive over this horizon. Let $BS(S, K, \sigma, r, q, t)$ denote the function relating the Black-Scholes model value $BS(S, K, \sigma, r, q, t) \in \mathbb{R}$ of a contingent claim to the underlying stock price level $S > 0$, the strike $K > 0$, the (constant) volatility $\sigma > 0$, calendar time $t \in [0, T]$, the constant interest rate r, and continuous dividend q. Let subscripts denote partial derivatives. We assume that the function $BS(S, K, \sigma, r, q, t)$ is governed by the Black-Scholes backward PDE. To make the notation easier, further in the expression $BS(S, K, \sigma, r, q, t)$ we will drop all variables not relevant to our particular context. Therefore, in this section we denote the function value as $BS(S, \sigma, t)$. With this notation, the corresponding Black-Scholes PDE reads (Hull 1997)

$$\frac{\partial BS(t,S,\sigma)}{\partial t} + (r-q)S\frac{\partial BS(t,S,\sigma)}{\partial S} + \frac{1}{2}\sigma^2 S^2 \frac{\partial^2 BS(t,S,\sigma)}{\partial S^2} = rBS(t,S,\sigma), \quad (1)$$

defined on some open region $\mathcal{R}$ of space and time. For example, for a European call or put, the region $\mathcal{R}$ would be the Cartesian product $\mathcal{R}_E \equiv [0, \infty) \times [0, T)$. As a second example, for a down-and-out call with a lower barrier $L \in (0, S_0)$, the region $\mathcal{R}$ would be the Cartesian product $\mathcal{R}_L \equiv (L, \infty) \times [0, T)$.

We furthermore assume that the Vega of the claim is always strictly positive, i.e., $BS_\sigma(S, \sigma, t) > 0$ on $\mathcal{R}$. This clearly holds for a European call or put on $\mathcal{R}_E$, but it can also be shown that it holds for a down-and-out call on $\mathcal{R}_L$. We also assume that one can directly observe

the market price $Z(T,K)$ of such a claim, and that this market price lies in some arbitrage-free open interval $\mathcal{A} \subset \mathbb{R}$. For a European call struck at K, $\mathcal{A}_C \equiv ((Q_T S - D_T K)^+, SQ_T)$, where $D_T = e^{-rT}$ is the discount factor, and $Q_T = e^{-qT}$ is the price appreciation factor. For a European put struck at K, $\mathcal{A}_P \equiv ((D_T K - Q_T S)^+, D_T K)$. For a down-and-out call struck at K, $\mathcal{A}_D \equiv ((D_T K - Q_T S)^+, Q_T(S - L))$ (Hull 1997).

For any such claim, we can implicitly define a function $\Sigma(S, t, K, T, r, q, Z)$ that relates the implied volatility Σ of the contingent claim to $(S, t) \in \mathcal{R}$ and to the market price of the contingent claim $Z \in \mathcal{A}$. Again, for ease of notation, we drop K, T, r, q from the list of independent variables, and then the definition of $\Sigma(S, t, Z)$ reads

$$BS(S, \Sigma(S,t,Z), t) = Z. \tag{2}$$

Let $\mathcal{D}$ denote the domain for this function, which is defined as the Cartesian product of $\mathcal{R}$ and $\mathcal{A}$. Since the PDE in Equation (1) holds for any level of $\sigma > 0$, it holds in particular if we set $\sigma = \Sigma(S, t, Z)$:

$$\left\{ \frac{\partial BS(t,S,\sigma)}{\partial t} + (r-q)S\frac{\partial BS(t,S,\sigma)}{\partial S} + \frac{1}{2}\sigma^2 S^2 \frac{\partial^2 BS(t,S,\sigma)}{\partial S^2} - rBS(t,S,\sigma) \right\}\Bigg|_{\sigma=\Sigma(S,t,Z)} = 0. \tag{3}$$

We now show that Equation (2) and Equation (3) can be used to generate a nonlinear PDE governing $\Sigma(S, t, Z)$ on $\mathcal{D}$.

First, differentiate Equation (2) with respect to t:

$$BS_t(S, \Sigma(S,t,Z), t) + BS_\sigma(S, \Sigma(S,t,Z), t)\Sigma_t(S,t,Z) = 0. \tag{4}$$

Second, differentiate Equation (2) with respect to S instead:

$$BS_S(S, \Sigma(S,t,Z), t) + BS_\sigma(S, \Sigma(S,t,Z), t)\Sigma_S(S,t,Z) = 0. \tag{5}$$

In what follows, we will also drop the three arguments of Σ for notational ease, as it shouldn't give rise to any confusion. Now differentiate Equation (5) with respect to S:

$$BS_{SS}(S,\Sigma,t) + 2BS_{S\sigma}(S,\Sigma,t)\Sigma_S + BS_{\sigma\sigma}(S,\Sigma,t)\Sigma_S^2 + BS_\sigma(S,\Sigma,t)\Sigma_{SS} = 0. \tag{6}$$

Substituting Equation (4) and Equation (6) into Equation (3) implies:

$$-BS_\sigma(S,\Sigma,t)\Sigma_t - \frac{1}{2}\Sigma^2 S^2 [2BS_{S\sigma}(S,\Sigma,t)\Sigma_S + BS_{\sigma\sigma}(S,\Sigma,t)\Sigma_S^2 + BS_\sigma(S,\Sigma,t)\Sigma_{SS}] + (r-q)SBS_S(S,\Sigma,t) = rBS(S,\Sigma,t). \tag{7}$$

We now show that we can express Vanna $BS_{S\sigma}(S, \Sigma, t)$ and Volga $BS_{\sigma\sigma}(S, \Sigma, t)$ in terms of Vega $BS_\sigma(S, \Sigma, t)$. First, differentiate Equation (2) with respect to Z:

$$BS_\sigma(S,\Sigma,t)\Sigma_Z = 1. \tag{8}$$

Next, differentiate Equation (8) with respect to S:

$$BS_{S\sigma}(S,\Sigma,t)\Sigma_Z + BS_{\sigma\sigma}(S,\Sigma,t)\Sigma_S\Sigma_Z + BS_\sigma(S,\Sigma,t)\cdot\Sigma_{SZ} = 0. \tag{9}$$

Now differentiate Equation (8) with respect to Z instead:

$$BS_{\sigma\sigma}(S,\Sigma,t)\Sigma_Z^2 + BS_\sigma(S,\Sigma,t)\Sigma_{ZZ} = 0. \tag{10}$$

Solving Equation (10) for Volga $BS_{\sigma\sigma}(S, \Sigma, t)$ yields

$$BS_{\sigma\sigma}(S,\Sigma,t) = -BS_\sigma(S,\Sigma,t)\frac{\Sigma_{ZZ}}{\Sigma_Z^2}. \tag{11}$$

Substituting Equation (11) into Equation (9) and solving for Vanna $BS_{S\sigma}(S, \Sigma, t)$ implies:

$$BS_{S\sigma}(S,\Sigma,t) = BS_\sigma(S,\Sigma,t)\frac{\Sigma_S}{\Sigma_Z^2}\Sigma_{ZZ} - BS_\sigma(S,\Sigma,t)\frac{\Sigma_{SZ}}{\Sigma_Z}. \tag{12}$$

Substituting Equation (11) and Equation (12) into Equation (7) yields

$$0 = BS_\sigma(S,\Sigma,t)\left\{\Sigma_t + \frac{1}{2}\Sigma^2 S^2\left[\left(\frac{\Sigma_S}{\Sigma_Z}\right)^2\Sigma_{ZZ} - 2\frac{\Sigma_S}{\Sigma_Z}\Sigma_{SZ} + \Sigma_{SS}\right]\right\} - (r-q)SBS_S(S,\Sigma,t) + rZ. \tag{13}$$

Also from Equation (8), we can express the option Vega via Σ_Z, from Equation (5)—the option Delta, and substitute these expressions into Equation (13) to obtain

$$0 = BS_\sigma(S,\Sigma,t)\left\{\Sigma_t + \frac{1}{2}\Sigma^2 S^2\left[\left(\frac{\Sigma_S}{\Sigma_Z}\right)^2 \Sigma_{ZZ} - 2\frac{\Sigma_S}{\Sigma_Z}\Sigma_{SZ} + \Sigma_{SS}\right] + (r-q)S\Sigma_S + rZ\Sigma_Z\right\}. \quad (14)$$

Therefore, if the option Vega is non-zero, the backward PDE for the implied volatility Σ finally takes the form

$$\Sigma_t + \frac{1}{2}\Sigma^2 S^2\left[\left(\frac{\Sigma_S}{\Sigma_Z}\right)^2 \Sigma_{ZZ} - 2\frac{\Sigma_S}{\Sigma_Z}\Sigma_{SZ} + \Sigma_{SS}\right] + (r-q)S\Sigma_S + rZ\Sigma_Z = 0. \quad (15)$$

This is a quasilinear[1] PDE of the parabolic type.

When the Black-Scholes model Delta of a contingent claim is known in closed form, there is an alternative quasilinear PDE that governs the function $\Sigma(S, Z, t)$ on $\mathcal{D}$. Solving Equation (8) for Vega $BS_\sigma(S,\Sigma,t)$, substituting the result into Equation (5), and then solving for Delta $BS_S(S,\Sigma,t)$ implies:

$$BS_S(S,\Sigma,t) = -\frac{\Sigma_S}{\Sigma_Z}. \quad (16)$$

Hence Equation (13) can also be written as:

$$\Sigma_t + \frac{1}{2}\Sigma^2 S^2\left[BS_S^2(S,\Sigma,t)\Sigma_{ZZ} + 2BS_S(S,\Sigma,t)\Sigma_{SZ} + \Sigma_{SS}\right] + (r-q)S\Sigma_S + rZ\Sigma_Z = 0. \quad (17)$$

To illustrate, it is well known that for a European Call, Delta $BS_S(S,\Sigma,t)$ is known in closed form:

$$BS_S(S,\Sigma,t) = N(d_1(S,\Sigma,t)), \quad (18)$$

where:

$$d_1(S,\Sigma,t) \equiv \frac{\ln\frac{S}{K} + \frac{\Sigma^2}{2}T}{\Sigma\sqrt{T}}, \quad (19)$$

and $N(x)$ is the normal CDF. Hence, for a European call, the quasilinear PDE Equation (17) can also be represented as another quasilinear PDE:

$$\Sigma_t + \frac{1}{2}\Sigma^2 S^2\left[N^2(d_1(S,\Sigma,t))\Sigma_{ZZ} + 2N(d_1(S,\Sigma,t))\Sigma_{SZ}^2 + \Sigma_{SS}\right] + (r-q)S\Sigma_S + rZ\Sigma_Z = 0, \quad (20)$$

whose domain is the Cartesian product of $\mathcal{R}_E$ and $\mathcal{A}_C$, which is $\mathcal{D} = (0,\infty) \times (0, T) \times ((Q_T S - D_T K)^+, Q_T S)$. Similar quasilinear PDE's can be derived for European puts or down-and-out calls.

For an American put option with a positive early exercise premium, in the continuation region the relevant PDE is Equation (15), since neither the value nor the Delta is known in closed form.

FORWARD EQUATION

In practice it is often necessary to simultaneously compute the Black-Scholes implied volatility of many options written on the same underlying, but having different strikes and maturity. This is to construct so-called the implied volatility surface, given market quotes $Z(K, T)$ and the market values of S, r, q. However, it is well-known that solving this problem by using the backward PDE is time-consuming since for every pair K, T a separate backward PDE has to be solved. In contrast, the forward equation can be used to do this efficiently in one sweep, see e.g., Dupire (1994) and Gatheral (2006).

Having this in mind, in this section we derive a forward PDE for the implied volatility $\Sigma(S, T, K, r, q, Z)$. For ease of notation, we will write it as $\Sigma(T, K, Z)$, thus dropping parameters that don't change. The derivation can be done in a way similar to that in the previous section. Therefore, here we will omit the detailed algebra, and just provide short explanations.

Again, we can start with the definition of the implied volatility $\Sigma(K, T, Z)$ in Equation (2), which in new variables read

$$BS(K,\Sigma(K,T,Z),T) = Z, \quad (21)$$

where $\Sigma(K, T, Z) \in [0,\infty)$, and the domain of definition for (K, T, Z) is $\mathcal{R}_{F,E} \equiv [0,\infty) \times (0,\infty) \times \mathcal{A}_C$.

To proceed, we need a forward PDE for the European option price $BS(K, T, \sigma)$ which is also known as Dupire's equation, Dupire (1994)

[1] A partial differential equation is said to be quasilinear if it is linear with respect to all the highest order derivatives of the unknown function (Pinchover and Rubinstein 2005).

$$\frac{\partial BS(K,T,\sigma)}{\partial T} = \frac{1}{2}\sigma^2(K)K^2\frac{\partial^2 BS(K,T,\sigma)}{\partial K^2} - (r-q)K\frac{\partial BS(K,T,\sigma)}{\partial K} - qBS(K,T,\sigma). \quad (22)$$

Since the PDE Equation (22) holds for any level of $\sigma > 0$, it holds, in particular, if we set $\sigma = \Sigma(K, T, Z)$. In what follows, we will drop the three arguments of Σ for notational ease.

Differentiating Equation (21) with respect to T, K and twice with respect to K yields

$$\begin{aligned} 0 &= BS_T(K,\Sigma,T) + BS_\sigma(K,\Sigma,T)\Sigma_T, \\ 0 &= BS_K(K,\Sigma,T) + BS_\sigma(K,\Sigma,T)\Sigma_K, \\ 0 &= BS_{KK}(K,\Sigma,T) + 2BS_{K\sigma}(K,\Sigma,T)\Sigma_K \\ &\quad + BS_{\sigma\sigma}(K,\Sigma,T)\Sigma_K^2 + BS_\sigma(K,\Sigma,T)\Sigma_{KK}. \end{aligned} \quad (23)$$

Substituting Equation (23) into Equation (22) implies:

$$\begin{aligned} 0 = BS_\sigma(K,\Sigma,T)\Sigma_T &- \frac{1}{2}\Sigma^2K^2\big[2BS_{K\sigma}(K,\Sigma,T)\Sigma_K \\ &+ BS_{\sigma\sigma}(K,\Sigma,T)\Sigma_K^2 + BS_\sigma(K,\Sigma,T)\Sigma_{KK}\big] \\ &+ (r-q)KBS_\sigma(K,\Sigma,T)\Sigma_K - qBS(K,\Sigma,T). \end{aligned} \quad (24)$$

Again, derivatives $BS_{K\sigma}(K, \Sigma, T)$ and $BS_{\sigma\sigma}(K, \Sigma, T)$ can be expressed in terms of $BS_\sigma(K, \Sigma, T)$. Differentiating Equation (21), first with respect to Z, and then with respect either to K, or to Z, yields

$$\begin{aligned} 1 &= BS_\sigma(K,\Sigma,T)\Sigma_Z, \\ 0 &= BS_{K\sigma}(K,\Sigma,T)\Sigma_Z + BS_{\sigma\sigma}(K,\Sigma,T)\Sigma_K\Sigma_Z \\ &\quad + BS_\sigma(K,\Sigma,T)\Sigma_{KZ}, \\ 0 &= BS_{\sigma\sigma}(K,\Sigma,T)\Sigma_Z^2 + BS_\sigma(K,\Sigma,T)\Sigma_{ZZ}. \end{aligned} \quad (25)$$

The last equation in this system can be solved for $BS_{\sigma\sigma}(K, \Sigma, T)$, and then the second one—for $BS_{K\sigma}(K, \Sigma, T)$. Substituting these solutions into Equation (24) yields

$$0 = BS_\sigma(K,\Sigma,T)\left\{\Sigma_T - \frac{1}{2}\Sigma^2K^2\left[\left(\frac{\Sigma_K}{\Sigma_Z}\right)^2\Sigma_{ZZ} - 2\frac{\Sigma_K}{\Sigma_Z}\Sigma_{KZ} + \Sigma_{KK}\right] + (r-q)K\Sigma_K\right\} - qZ. \quad (26)$$

Using the first line in Equation (25), this could be rewritten as

$$0 = BS_\sigma(K,\Sigma,T)\left\{\Sigma_T - \frac{1}{2}\Sigma^2K^2\left[\left(\frac{\Sigma_K}{\Sigma_Z}\right)^2\Sigma_{ZZ} - 2\frac{\Sigma_K}{\Sigma_Z}\Sigma_{KZ} + \Sigma_{KK}\right] + (r-q)K\Sigma_K - qZ\Sigma_z\right\}. \quad (27)$$

If the option Vega is non-zero, we finally obtain the forward PDE for the implied volatility $\Sigma(K, T, Z)$

$$\begin{aligned} 0 = \Sigma_T &- \frac{1}{2}\Sigma^2K^2\left[\left(\frac{\Sigma_K}{\Sigma_Z}\right)^2\Sigma_{ZZ} - 2\frac{\Sigma_K}{\Sigma_Z}\Sigma_{KZ} + \Sigma_{KK}\right] \\ &+ (r-q)K\Sigma_K - qZ\Sigma_Z. \end{aligned} \quad (28)$$

This PDE has to be solved subject to some initial and boundary conditions which are discussed in the next section.

Since we consider the European options, the Black-Scholes model strike Delta of a contingent claim is known in closed form. Then, similar to the previous section, the PDE in Equation (28) could be slightly simplified. Indeed, as follows from the second line of Equation (23) and first line of Equation (25)

$$BS_K(S,\Sigma,T) = -\frac{\Sigma_K}{\Sigma_Z}. \quad (29)$$

Hence Equation (28) can also be rewritten as:

$$\begin{aligned} 0 = \Sigma_T &- \frac{1}{2}\Sigma^2K^2\big[BS_K^2(K,\Sigma,T)\Sigma_{ZZ} \\ &+ 2BS_K(K,\Sigma,T)\Sigma_{KZ} + \Sigma_{KK}\big] + (r-q)K\Sigma_K - qZ\Sigma_Z. \end{aligned} \quad (30)$$

For instance, for a European call, the strike Delta $BS_K(K, \Sigma, T)$ can be found in closed form. Indeed, since the Black-Scholes European call option price is a homogeneous function of order 1 in (S, K), it is easy to find that

$$\begin{aligned} KBS_K(K,\sigma,T) &= BS(K,\sigma,T) - SBS_S(K,\sigma,T) \\ &= -Ke^{-rT}N(d_2(K,\sigma,T)), \end{aligned} \quad (31)$$

where $d_2 = d_1 - \sigma\sqrt{T}$.

INITIAL AND BOUNDARY CONDITIONS

The nonlinear PDE Equation (28) describes evolution of the function $\Sigma(K, T, Z) \in [0, \infty)$ at the domain $\mathcal{R}_{F,E}$, and has to be solved subject to some initial and boundary conditions. However, this immediately introduces some problems.

Indeed, the initial condition for Equation (28) has to be set at $T = 0$. From the Black-Scholes formula we know that the option Vega $BS_\sigma(K, \Sigma, T)$ vanishes at $T = 0$. Therefore, the expression in curly braces in Equation (26) could have any value. Also, the equation $BS_\sigma(K, \Sigma, T) = 0$ doesn't have a solution for Σ. This is because at $T = 0$ function $BS(K, \Sigma, 0)$ gets its intrinsic value (e.g. for the call option—$BS(K, \Sigma, 0) = (S - K)^+$), which doesn't depend on Σ. Accordingly, for the ITM options there is no Σ that would make the intrinsic value zero, and for the OTM options any Σ could be chosen.

To resolve this, we make a change of the dependent variable $\Sigma(K,T,Z) \mapsto \mathfrak{S}(K,T,Z) = \Sigma(K,T,Z)\sqrt{T}$. This pursues two goals. First, at $T = 0$, a natural initial condition implies $\mathfrak{S}(K, 0, Z) = 0$. Second, if we know $\mathfrak{S}(K, T, Z)$ given some values of (K, T, Z), the value of $\Sigma(K, T, Z)$ can be easily restored.

The forward PDE for the new dependent variable $\mathfrak{S}(K, T, Z)$ can be derived from Equation (28), which yields

$$\mathfrak{S}_T = \frac{1}{2T}\mathfrak{S}^2K^2\left[\left(\frac{\mathfrak{S}_K}{\mathfrak{S}_Z}\right)^2\mathfrak{S}_{ZZ} - 2\frac{\mathfrak{S}_K}{\mathfrak{S}_Z}\mathfrak{S}_{KZ} + \mathfrak{S}_{KK}\right] - (r-q)K\mathfrak{S}_K + qZ\mathfrak{S}_Z + \frac{1}{2T}\mathfrak{S}. \quad (32)$$

Since Equation (32) is a 2D parabolic PDE (quasi-linear), the boundary conditions must be set $\forall T > 0$.

Suppose that we consider a European call defined at the domain Ω: $[K, Z] \in [0, \infty] \times ((Q_T S - D_T K)^+, Q_T S)$ which is depicted in Exhibit 1. Special attention should be paid to two of these boundaries: $Z = 0$ and $Z = Q_T S - D_t K$—to decide whether the PDE needs any boundary condition at them.

As mentioned in Itkin and Carr (2011), the correct boundary conditions are determined by the speed of the diffusion term as we approach the boundary in a direction normal to the boundary. To illustrate, consider a PDE

$$C_t = a(x)C_{xx} + b(x)C_x + c(x)C, \quad (33)$$

EXHIBIT 1
The Domain Ω:$[K, Z] \in [0, \infty] \times \mathcal{A}_C$

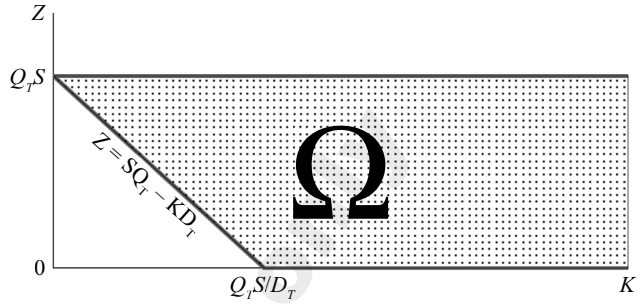

where $C = C(t, x)$ is some function of the time t and the independent variable $x \in [0, \infty)$, $a(x)$, $b(x)$, $c(x) \in C^2$ are some known functions of x. Then, as shown by Oleinik and Radkevich (1973), no boundary condition is required at $x = 0$ if $\lim_{x\to 0}[b(x) - a_x(x)] \geq 0$. In other words, the convection term at $x = 0$ is flowing upwards and dominates, as compared with the diffusion term. A well-known example of such consideration is the Feller condition as applied to the Heston model, see, e.g., Lucic (2008).

To make it clear, no boundary condition means that instead of the boundary condition at $x \to 0$, the PDE itself should be used at this boundary with coefficients $a(0)$, $b(0)$, $c(0)$.

In a later section, we show how to solve Equation (32) by using temporal discretization that gives rise to the following equation

$$\mathfrak{S}_T = \frac{1}{2T}\tilde{\mathfrak{S}}^2K^2\left[\left(\frac{\tilde{\mathfrak{S}}_K}{\tilde{\mathfrak{S}}_Z}\right)^2\mathfrak{S}_{ZZ} - 2\frac{\tilde{\mathfrak{S}}_K}{\tilde{\mathfrak{S}}_Z}\mathfrak{S}_{KZ} + \mathfrak{S}_{KK}\right] - (r-q)K\mathfrak{S}_K + qZ\mathfrak{S}_Z + \frac{1}{2T}\mathfrak{S}. \quad (34)$$

Here $S = S(T + \Delta T, K, Z)$, $\tilde{\mathfrak{S}} = \tilde{\mathfrak{S}}(T, K, Z)$, and ΔT is the step of the temporal grid in T. Equation (34) is a linear PDE since all coefficients are already known (they are either given, e.g., r, q, T, or known from the previous time step). Thus, Equation (34) is a 2D version of Equation (33).

Accordingly, in the K direction with allowance for Equation (23), Equation (31), the condition $\lim_{K\to 0} b(K) - a'(K) \geq 0$ reads

$$\lim_{K\to 0}\left[b(K)-a'(K)\right]$$
$$=\lim_{K\to 0}\left\{-\left[(r-q)K+\frac{\tilde{\mathfrak{S}}K}{T}\left(\tilde{\mathfrak{S}}+K\tilde{\mathfrak{S}}_K\right)\right]\right\}$$
$$=\lim_{K\to 0}\left\{-K\left[r-q+\frac{\tilde{\mathfrak{S}}}{T}\left(\tilde{\mathfrak{S}}-K\sqrt{T}\,\frac{BS_K(K,\Sigma,T)}{BS_\sigma(K,\Sigma,T)}\right)\right]\right\}$$
$$=\lim_{K\to 0}\left\{-K\left[r-q+\frac{\tilde{\mathfrak{S}}}{T}\left(\tilde{\mathfrak{S}}+\frac{N(d_2(K,\sigma,T))}{\Phi(d_2(K,\Sigma,T))}\right)\right]\right\}=0,$$
$$\Phi(x)=N'(x),$$

because $\lim_{K\to 0}\tilde{\mathfrak{S}}(K,T,Z)=0,\ T>0$. Therefore, as per Oleinik and Radkevich (1973), no boundary condition should be set at $K=0$, as the PDE itself serves as the correct boundary condition.

However, our domain Ω includes the only point with $K=0$, while the left boundary is a line $Z=Q_TS-D_TK$. It can be easily checked that along this line S = 0, which is the required boundary conditions.

In the Z direction, again using Equation (25), we obtain

$$\frac{1}{2}K^2\frac{\partial}{\partial Z}\left(\frac{\tilde{\mathfrak{S}}\tilde{\mathfrak{S}}_K}{\tilde{\mathfrak{S}}_Z}\right)^2=K^2\frac{\tilde{\mathfrak{S}}\tilde{\mathfrak{S}}_K^2}{\tilde{\mathfrak{S}}_Z}\left(1+\frac{\tilde{\mathfrak{S}}\tilde{\mathfrak{S}}_{KZ}}{\tilde{\mathfrak{S}}_Z\tilde{\mathfrak{S}}_K}-\frac{\tilde{\mathfrak{S}}\tilde{\mathfrak{S}}_{ZZ}}{\tilde{\mathfrak{S}}_Z^2}.\right)$$
$$=K^2T\frac{\tilde{\Sigma}\tilde{\Sigma}_K^2}{\tilde{\Sigma}_Z}\left(1+\frac{\tilde{\Sigma}\tilde{\Sigma}_{KZ}}{\tilde{\Sigma}_Z\tilde{\Sigma}_K}-\frac{\tilde{\Sigma}\tilde{\Sigma}_{ZZ}}{\tilde{\Sigma}_Z^2}\right)$$
$$=K^2T\frac{\tilde{\Sigma}\tilde{\Sigma}_K^2}{\tilde{\Sigma}_Z}\left(1+\tilde{\Sigma}\frac{BS_{K,\sigma}(K,\tilde{\Sigma},T)}{BS_K(K,\tilde{\Sigma},T)}\right)$$
$$=K^2T\frac{\tilde{\Sigma}\tilde{\Sigma}_K^2}{\tilde{\Sigma}_Z}\left(1-\tilde{\Sigma}\frac{BS_{\sigma,K}(K,\tilde{\Sigma},T)}{D_TN(d_2(K,\tilde{\Sigma},T))}\right)$$
$$=K^2T\frac{\tilde{\Sigma}\tilde{\Sigma}_K^2}{\tilde{\Sigma}_Z}\left(1-\tilde{\Sigma}\frac{\Phi(d_2(K,\tilde{\Sigma},T))d_1(K,\tilde{\Sigma},T)}{D_TN(d_2(K,\tilde{\Sigma},\mathrm{T}))}\right)\tag{35}$$

From Equation (25), $\Sigma_Z=1/BS_\sigma(K,\tilde{\Sigma},T)>0$. Therefore,

$$\lim_{Z\to 0}\left[b(Z)-a'(Z)\right]=\lim_{Z\to 0}\left[qZ-K^2\frac{\tilde{\Sigma}\tilde{\Sigma}_K^2}{\tilde{\Sigma}_Z}\left(1-\tilde{\Sigma}\frac{\Phi(d_2(K,\tilde{\Sigma},T))d_1(K,\tilde{\Sigma},T)}{D_TN(d_2(K,\tilde{\Sigma},T))}\right)\right]$$
$$=-K^2\lim_{Z\to 0}\left[\tilde{\Sigma}\tilde{\Sigma}_K^2BS_\sigma(K,\tilde{\Sigma},T)\left(1-\tilde{\Sigma}\frac{\Phi(d_2(K,\tilde{\Sigma},T))d_1(K,\tilde{\Sigma},T)}{D_TN(d_2(K,\tilde{\Sigma},T))}\right)\right]$$

EXHIBIT 2

AQ2

Implied Volatility $\mathfrak{S}$ Obtained by Solving the Equation $Z=0$ for the European Call Option

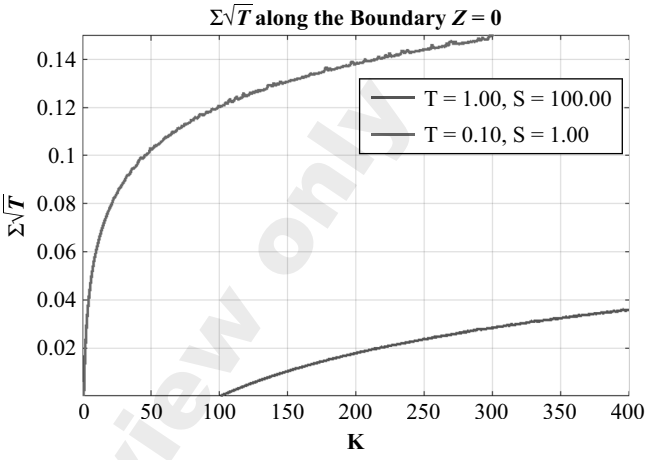

Since at $Z=0$, the domain Ω is a straight line $KD_T\geq SQ_T$, it can be checked that the value of $d_1(K,\tilde{\Sigma},T)$ along this line is always negative, while $\tilde{\Sigma}\neq 0$ except the point $K=SQ_T/D_T$. Therefore, what remains to be checked is the behavior of the option Vega as $Z\to 0$. The implied volatility $\tilde{\Sigma}$, which solves the equation $Z=0$, can be found numerically, and is not zero at $KD_T>SQ_T$. Therefore, Vega is positive (although it is very small). Thus, $\lim_{Z\to 0}[b(Z)-a'(Z)]<0$. Therefore, as per Oleinik and Radkevich (1973), we need a boundary condition at the boundary $Z=0$. This condition can be found by solving the equation

$$Z=BS(K,\Sigma,T)=0,\tag{36}$$

with respect to Σ. A typical example of the behavior of this solution is given in Exhibit 2, which is computed using the following input data: $r=0.02$, $q=0.01$, and two cases with ($S=1.0$, $T=0.1$) and ($S=100$, $T=1.0$).

Boundary conditions at $K\to\infty$. To set this boundary condition, we need to know an asymptotic behavior of the implied volatility when $K\to\infty$. This was a subject of intensive research for the last decade, and

several useful results are available in the literature, see, e.g., Lee (2004); Benaim and Friz (2009); Gulisashvili (2010) and references therein. In particular, the following asymptotic formula was obtained in Gulisashvili (2010)

$$\mathfrak{S}(K) = \sqrt{2}\left[\sqrt{\log\frac{K}{F} + \log\frac{SQ_T}{C(K)}} - \sqrt{\log\frac{SQ_T}{C(K)}}\right] + O\left(\left(\log\frac{SQ_T}{C(K)}\right)^{-1/2}\log\log\frac{SQ_T}{C(K)}\right), \quad (37)$$

as $K \to \infty$. Here, $C(K)$ is the call option price corresponding to the given K, T, and $F = SQ_t/D_T$ is the forward price. One can observe, that in our case $C(K) = Z$. Therefore, as the boundary condition at $K \to \infty$ we can use

$$\mathfrak{S}(K) = \sqrt{2}\left[\sqrt{\log\frac{K}{F} + \log\frac{SQ_T}{Z}} - \sqrt{\log\frac{SQ_T}{Z}}\right]. \quad (38)$$

Since $Z \leq SQ_T$, the logarithm $\log(SQ_T/Z)$ is always non-negative.

However, this asymptotics cannot be used along the whole vertical line of the domain Ω at $K \to \infty$ in Exhibit 1. For instance, at $Z = SQ_T$, the remainder of the approximation in Equation (37) is large. In this case, one can solve numerically the equation

$$BS(K, \mathfrak{S}, T) = Z. \quad (39)$$

Boundary conditions at $Z = SQ_T$. The condition $Z = Q_T S$ implies that $N(d_1(K, T, \mathrm{S})) = 1$ and $N(d_2(K, T, \mathrm{S})) = 0$. This means that $\mathrm{S} \to \infty$. To resolve this when constructing a numerical solution, one can move this boundary to $Q_T(S - \Delta S)$, where $\Delta S \ll S$. Then, using a Taylor series expansion of $BS(K, \mathrm{S}, T)$ around $\mathrm{S} \to \infty$, we can find the solution of the equation

$$BS(K, \mathfrak{S}, T) = Q_T(S - \Delta S). \quad (40)$$

Taking into account first eight terms in this expansion, we arrive at the following equation

$$0 = \sqrt{2k}[-6(\mathfrak{S}^2 - 20)\log^4(k) + 24(\mathfrak{S}^4 - 12\mathfrak{S}^2 + 240)\log^2(k) + \log^6(k) - 48(\mathfrak{S}^6 - 4\mathfrak{S}^4 + 48\mathfrak{S}^2 - 960)] + 24\sqrt{\pi}\delta e^{\frac{\mathfrak{S}^2}{8}}\mathfrak{S}^7, \quad (41)$$

where $k = SQ_T/(KD_T)$, $\delta = \Delta SQ_T/(KD_T)$, so $\delta \ll k$. This equation has three roots, and usually one is negative. Among the other two positive roots, we need the smallest one, which approximately corresponds to the solution of Equation (41) with $\delta = 0$. Then this root aligns with the asymptotics of the solution at large K considered in the previous paragraph. Setting $\delta = 0$ in Equation (41) gives rise to a cubic algebraic equation that can be solved analytically. Alternatively, Equation (40) can be solved numerically.

ANOTHER TYPE OF PDE

The Equation (32) can be further transformed into another type of the PDE. Indeed, the expression in square brackets in Equation (32) can be represented as

$$A(T, K, Z, \mathfrak{S}) = \left(\frac{\mathfrak{S}_K}{\mathfrak{S}_Z}\right)^2 \mathfrak{S}_{ZZ} - 2\frac{\mathfrak{S}_K}{\mathfrak{S}_Z}\mathfrak{S}_{KZ} + \mathfrak{S}_{KK} = \mathfrak{S}_Z\left[\frac{\partial\left(\frac{\mathfrak{S}_K}{\mathfrak{S}_Z}\right)}{\partial K} - \frac{1}{2}\frac{\partial\left(\frac{\mathfrak{S}_K}{\mathfrak{S}_Z}\right)^2}{\partial Z}\right]. \quad (42)$$

From Equation (29), and Equation (31) we have

$$\frac{\mathfrak{S}_K}{\mathfrak{S}_Z} = -BS_K(S, \mathfrak{S}, T) = e^{-rT}N(d_2(K, \mathfrak{S})), \quad (43)$$

Substituting Equation (43) into Equation (42), and taking into account that $\mathrm{S} = \mathrm{S}(K, T, Z)$, we obtain

$$\begin{aligned} A(T, K, Z) &= a(T, K, \mathfrak{S})\mathfrak{S}_Z \\ &\quad [b(T, K, \mathfrak{S})\mathfrak{S}_Z + c(T, K, \mathfrak{S})\mathfrak{S}_K + d(T, K, \mathfrak{S})], \\ a(T, K, \mathfrak{S}) &= \frac{1}{\sqrt{2\pi}}\exp\left(-rT - \frac{1}{2}d_2(K, \mathfrak{S})^2\right), \\ c(T, K, \mathfrak{S}) &= \frac{\partial d_2(K, \sigma, T)}{\partial \sigma}\Big|_{\sigma\sqrt{T}=\mathfrak{S}}, \\ b(T, K, \mathfrak{S}) &= -e^{-rT}N(d_2(K, \mathfrak{S}))c(T, K, \mathfrak{S}), \\ d(T, K, \mathfrak{S}) &= \frac{\partial d_2(K, \sigma, T)}{\partial K}\Big|_{\sigma\sqrt{T}=\mathfrak{S}}. \end{aligned} \quad (44)$$

With this expressions, the PDE in Equation (32) takes the form

$$\mathfrak{S}_T = \frac{a(T,K,\mathfrak{S})K^2}{2T}\mathfrak{S}^2\mathfrak{S}_Z$$
$$[b(T,K,\mathfrak{S})\mathfrak{S}_Z + c(T,K,\mathfrak{S})\mathfrak{S}_K + d(T,K,\mathfrak{S})]$$
$$-(r-q)K\mathfrak{S}_K + qZ\mathfrak{S}_Z + \frac{1}{2T}\mathfrak{S}. \quad (45)$$

In contrast to Equation (32), this is a nonlinear *hyperbolic* PDE. It can be used as an alternative to Equation (32), which is a quasilinear *parabolic* PDE. Accordingly, the PDE in Equation (45) requires just the boundary conditions at lines $K \in [SQ_T/D_T, \infty)$ and $Z = (SQ_T - D_T K)^+$, see Exhibit 1.

Equation (45) can be further simplified by using Equation (43), which yields

$$\mathfrak{S}_T = -\Theta(T,K,\sigma)\big|_{\sigma\sqrt{T}=\mathfrak{S}}\ \mathfrak{S}_Z + \frac{1}{2T}\mathfrak{S}, \quad (46)$$

where $\Theta(T,K,\sigma)$ is the option Theta. This, of course, also follows from Equation (23) and Equation (25), so Equation (46) can be obtained directly from these equations. Equation (32) is a one-dimensional nonlinear PDE, with K being a dummy variable. In other words, for any fixed K, this is a one-dimensional nonlinear PDE, with T and Z being the independent variables.

THE PDEs AND NUMERICAL SOLUTIONS—CONNECTION TO PHYSICS

In the last section of this article, we will describe our numerical method, which is needed to solve either the PDE in Equation (32) or in Equation (45). The method consists of two basic steps:

1. To deal with the nonlinear part of the PDE, we use a version of the fix-point Picard iteration algorithm, which relies on the Banach fixed-point theorem, Granas and Dugundji (2003).
2. Then, to solve the linear PDE, at every iteration we use a splitting technique, see Lanser and Verwer (1999); Duffy (2006); Itkin (2017b), and references therein.

With regard to the first step, we have to mention that quasilinear parabolic PDEs, despite not being in exactly the same form as in Equation (34), are known in the physics literature. For instance, G. Kirchhoff in Kirchhoff (1883) proposed the hyperbolic integro-differential equation in order to describe small, transversal vibrations of an elastic string of length l (at rest) when the longitudinal motion can be considered negligible with respect to the transversal one. Then in Gobbino (1999) and Nakao (2009), the authors deal with some generalized degenerate Kirchhoff equations of the form

$$u_t = (1+\|\nabla u\|^2_{L^2(\Omega)})\Delta u,$$

which is a quasilinear parabolic PDE. Solution of this equation is considered, e.g., in Dawidowski (2017) by using the fixed-point theorem. As it will be seen below, this is also our preferred approach in this article.

More general, a non-degenerate quasilinear parabolic PDEs on a junction, satisfying a nonlinear Neumann boundary condition at the junction point $x = 0$ was considered in Wahbi (2018)

$$\partial_t u_i(t,x) = \sigma_i(x,\partial_x u_i(t,x))\partial^2_{x,x} u_i(t,x)$$
$$+ H(x,u_i(t,x),\partial_x u_i(t,x)), \quad \forall x > 0, i \in [1,...,I],$$
$$0 = F\big(u(t,0),\partial_x u_i(t,0)\big).$$

The Kirchhoff law corresponds to the case where function F is linear in $\partial_x u_i(t,x)$ and independent of u. As explained in Nikol'skii (1953), the main motivations for this are applications in physics, chemistry, and biology (for instance small transverse vibrations in a grid of strings, vibration of a grid of beams, drainage system, electrical equation with Kirchhoff's law, wave equation, heat equation, etc.).

We can also mention a paper of one of the authors, Itkin (2018), where the fixed point method is used to solve similar nonlinear parabolic PDEs. Those PDEs arise when solving some optimization problems in finance (despite the fact that they are much simpler than those considered in this article).

As far as the second step is concerned, it turns out that splitting was first proposed for solving some problems in physics. Therefore, we provide a short historical overview with the aim of revealing and emphasizing this connection. In so doing, we want to put a brick into a wide bridge between the methods of physics and those of mathematical/computational finance.

By definition, splitting is a numerical method for solving differential equations in several steps such that at every step, only some part of the whole differential

operator is used. Therefore, the solution of the PDE is split into several step, and at every step, a simpler problem should be solved, as compared with the original problem. Nowadays, this terminology is extended by introducing the ADI (alternative direction implicit), the ADE (alternative direction explicit), and the LOD (locally one dimensional) methods. Actually, they all are pretty similar in a sense that they exploit the same idea, with a few minor differences, namely:

- At every step, the ADI might take into account the PDE terms in various dimensions, two of them, for instance. But one dimension is considered as known (i.e., the corresponding terms are approximated at the previous time step), while the other are unknown (and, thus, they correspond to the current time). The scheme is written as implicit, i.e., it requires solving a system of linear equations at every step of splitting.
- The ADE scheme is similar to ADI with regard to splitting, but results in the explicit scheme.
- The LOD scheme at every step uses just the PDE terms in one direction (except for the mixed derivative terms).

For more detail, see, e.g., Roach (1976); Duffy (2006); Glowinski, Pan, and Tai (2016).

The main advantage of this technique is the variability of numerical methods that can be used at every step of splitting. For instance, the splitting can be done by dimensions (so, in case of a parabolic PDE, the step dealing with the one-dimensional diffusion operators can use a different numerical method, as compared with the step for the mixed derivative term, for example), or by physical processes (so, the convection term could be treated in a separate step from the diffusion term, and then each step could use an appropriate numerical method), and so forth.

The first steps in this direction were done for PDEs that described multidimensional diffusion with no mixed derivatives and no convection terms. The classical papers on this subject are Douglas, Jr. and Rachford, Jr. (1956) and Peaceman and Rachford, Jr. (1955). However, these schemes cannot be directly applied to solving many real CFD and hydrodynamic problems, as the latter do include convection and mixed derivatives terms.

The work on generalization of splitting for such problems was led in parallel by the USSR and Western scientists. Apparently, the first discoveries on this technique, which were further elaborated into a systematic approach, were made in the USSR. However, this is not well-known in the West. Around the 1960s, this technique, called the method of fractional steps, was introduced by Russian applied physicists and mathematicians in response to a high demand in rocket science for solving multidimensional problems of hydro and fluid dynamics and theoretical mechanics. Perhaps, the best-known works of that period in this field are Yanenko (1971, the Russian version was published in 1967 and then translated by Springer-Verlag in 1971), Dyakonov (1964, in Russian), and Samarski (1964). In particular, the editor's preface to Yanenko (1971) says, "The method of fractional steps, known familiarly as the method of splitting, is a remarkable technique, developed by N. N. Yanenko and his collaborators, for solving problems in theoretical mechanics numerically. It is applicable especially to potential problems, problems of elasticity and problems of fluid dynamics. Most of the applications at the present time have been to incompressible flow with free boundaries and to viscous flow at low speeds. The method offers a powerful means of solving the Navier-Stokes equations and the results produced so far cover a range of Reynolds numbers far greater than that attained in earlier methods. Further development of the method should lead to complete numerical solutions of many of the boundary layer and wake problems which at present defy satisfactory treatment".

Since Russian scientific papers were published in the West with a delay of four to five years (if they were ever published in the West at all), some of these methods have been rediscovered. For instance, in 1968, Gilbert Strang published his seminal paper, which, based on the modern terminology, belongs to the LOD schemes (Strang 1968). Another popular ADI scheme, named after Craig and Sneyd (1988), is actually a version of Samarski (1964). To illustrate this, we want to share a story of our friend and colleague Dr. Daniel Duffy, who is the author of a nice book about a FD approach in finance, Duffy (2006), which also describes various aspects of splitting.

When Daniel studied at university, he had a supervisor who was a friend of G. Marchuk and also a former student of G. Strang. The supervisor wanted Daniel to fly to Novosibirsk, Siberia, where both N. Yanenko and G. Marchuk worked at that time: academician Yanenko was the Director of the Institute

of Theoretical and Applied Mechanics of the Siberian Division of the USSR Academy of Sciences, and academician Marchuk was the President of the USSR Academy of Sciences. Unfortunately, that was the period of the Cold War, so Daniel missed this opportunity. Instead, he went to Paris. And since he could read Russian a bit, he searched through the French second-hand book stores to find some papers on physics and mathematics. Surprisingly, he found some Russian versions of the mathematical journals, as well as some books, and sometimes even discovered their translation into English. These sources also contained papers about splitting. That is how he learned about it, and later in his book, Duffy (2006), he correctly reflected on the contributions of the Russian scientists to the field.

As far as the ADE method is concerned, the classical book on this subject was written by V. Saul'yev Saul'yev (1964; in the USSR it was published in 1960, and in fact, one of the authors, AI, is his former student and still has a hard copy in his library). These methods were subsequently applied to a range of problems in hydrology, soil mechanics, heat transfer, and wave propagation, see Pealat and Duffy (2011) and references therein. However, with the development of ADI, those methods were treated as inefficient, as they set some restrictive conditions on the time step of the numerical method, although they are highly suitable for parallelization. Later, this conclusion was partly re-considered, again see Pealat and Duffy (2011). They show that in contrast to traditional time-marching schemes such as Crank–Nicolson and implicit Euler, the ADE method discretizes the ODE in such a way that the solution can be computed as the average of two unconditionally stable explicit schemes. The method scales to n-factor PDEs and can be seen as an example of an additive operator splitting (AOS) method, which solves ODE systems as the sum of a number of simpler problems.

Another branch, the ADI methods, received closer attention over time. Among various papers we can mention a work of In't Hout and Welfert (2007); In't Hout and Foulon (2010); Haentjens and In't Hout (2012), and also references therein.

Nowadays, splitting is still a powerful tool of numerical mathematics and is heavily used in various applications related to different areas of science, including computational finance. Historically, there is a clear bridge between physics and finance. With this emphasis, in the next section we describe splitting as applied to our problem in more detail.

NUMERICAL METHOD

In this section, we describe a numerical method used to solve either the PDE in Equation (32) or in Equation (45). The method is constructed similar to how this is done in Itkin (2018).

First, we rewrite Equation (32) and Equation (45) in the operator form by introducing an operator $\mathcal{L}(T,K,Z):[0,\infty)\mapsto[0,\infty)$. With this notation, Equation (32) can be represented as

$$\mathfrak{S}_T=\mathcal{L}(T,K,Z)\mathfrak{S}, \tag{47}$$

where

$$\mathcal{L}(T,K,Z)=\frac{1}{2T}\mathfrak{S}^2K^2\left[\left(\frac{\mathfrak{S}_K}{\mathfrak{S}_Z}\right)^2\partial_Z^2-2\frac{\mathfrak{S}_K}{\mathfrak{S}_Z}\partial_K\partial_Z+\partial_K^2\right] -(r-q)K\partial_K+qZ\partial_Z+\frac{1}{2T}, \tag{48}$$

Similarly, Equation (45) can be rewritten in the same form with

$$\mathcal{L}(T,K,Z)=\frac{a(K,T,Z)K^2}{2T}\mathfrak{S}^2\mathfrak{S}_Z[b(K,T,Z)\partial_Z +c(K,T,Z)\partial_K+d(K,T,Z)] -(r-q)K\partial_K+qZ\partial_Z+\frac{1}{2T}. \tag{49}$$

Suppose we now discretize the time to maturity $T\in[0,\infty)$ by creating a uniform grid in time with step ΔT, so our discrete time is defined at the points $[0,\Delta T, 2\Delta T,\ldots)$. By using Taylor series expansion, it can be shown that the discrete solution of the Equation (47) up to $O((\Delta T))$ could be represented in the form

$$\mathfrak{S}(T+\Delta T,K,Z)=e^{\Delta T\mathcal{L}(T,K,Z)}\ \mathfrak{S}(T,K,Z) \tag{50}$$

where $e^{\Delta T\mathcal{L}(T,\,K,\,Z)}$ is the operator exponent, Hochschild (1981).

Again, using the Taylor series expansion, one can verify that the following scheme

$$\mathfrak{S}(T+\Delta T,K,Z)=e^{\Delta T\mathcal{L}(T+\Delta T,K,Z)}\mathfrak{S}(T,K,Z) \tag{51}$$

also approximates Equation (47) up to in $O((\Delta T))$. Combining them together, we obtain the scheme

$$\mathfrak{S}(T+\Delta T,K,Z)=e^{\frac{1}{2}\Delta T[\mathcal{L}(T+\Delta T,K,Z)+\mathcal{L}(T,K,Z)]}\mathfrak{S}(T,K,Z), \tag{52}$$

which approximates Equation (47) up to $O((\Delta T)^2)$.

Now we setup an iterative algorithm to solve this discrete equation. This algorithm is a version of the fix-point Picard iteration algorithm, and relies on the Banach fixed-point theorem, Granas and Dugundji (2003):

1. At the first iteration, we start by setting $\mathcal{L}(T+\Delta T,K,Z)=\mathcal{L}(T,K,Z)$ as the initial guess. Thus, Equation (52) transforms to Equation (50), which could be represented in the form

$$\mathfrak{S}^{(1)}(T+\Delta T,K,Z)=e^{\Delta T\mathcal{L}(T,K,Z)}\mathfrak{S}(T,K,Z), \tag{53}$$

   where in $\mathfrak{S}^{(k)}$ the superscript $^{(k)}$ marks the value of $\mathfrak{S}$ found at the k-th iteration of the numerical procedure. As the exponent $\mathcal{L}(T,K,Z)$ in the right hands side of Equation (53) is computed at the known time T, it is a *linear* operator with coefficients being the known functions of (K,T,Z). In particular, when $T=0$, these functions are determined by the initial condition. If $T>0$, they are determined by the solution at the previous time step.

   Equation (53) could be solved by either computing the discrete matrix exponential defined on some grid in (K,Z) (which could be done with complexity $O(N^3M+NM^3)$, N is the number of the grid points in K direction, and M is the number of the grid points in Z direction), or by using any sort of Padé approximation of the exponential operator. For instance, the Padé approximation (1, 1) leads to the well-known Crank-Nicholson scheme, which could be solved with the linear complexity in N and M, and provides $O((\Delta T)^2)$ approximation in time, see Itkin (2017b).
2. To proceed, we represent Equation (52) in the form

$$\mathfrak{S}^{(k)}(T+\Delta T,K,Z)=e^{\frac{1}{2}\Delta T\left[\mathcal{L}^{(k-1)}(T+\Delta T,K,Z)+\mathcal{L}(T,K,Z)\right]}\mathfrak{S}^{(k-1)}(T,K,Z),\qquad k>1. \tag{54}$$

   Therefore, the next approximation $\mathfrak{S}^{(k)}(T+\Delta T,K,Z)$ to $\mathfrak{S}(T+\Delta T,K,Z)$ can be found again by either computing the matrix exponential, or by using some Padé approximation.

Having this machinery in hand, we can proceed in the same manner until the entire procedure converges, i.e., when the condition

$$\|\mathfrak{S}^{(k)}(T+\Delta T,K,Z)-\mathfrak{S}^{(k-1)}(T+\Delta T,K,Z)\|<\varepsilon$$

is reached after k iterations, with ε being the method tolerance, and $\|\cdot\|$ being some norm, e.g., L^2.

Note, that Equation (54) with the accuracy $O((\Delta T)^2)$ can be rewritten in the form

$$\begin{aligned}\mathfrak{S}_T^{(k)}&=\frac{1}{2}[\mathcal{L}(T,K,Z)+\mathcal{L}^{(k-1)}(T+\Delta T,K,Z)]\mathfrak{S}^{(k-1)}\\&=\tilde{\mathcal{L}}^{(k-1)}\mathfrak{S}^{(k-1)},\end{aligned} \tag{55}$$

where tilde in the new notation $\tilde{\mathcal{L}}^{(k-1)}$ means that we take a half of sum of the operators L at times T and $T+\Delta T$, and $(k-1)$ means that at time level $T+\Delta T$ we take the value of the operator at the $(k-1)$-th iteration.

Coordinate Transformation

Since our PDEs are defined in the domain Ω, which has a trapezoidal shape, we cannot directly apply a finite-difference (FD) method for solving Equation (54), while finite elements or Radial Basis Functions methods can be used here with no problem. However, a simple trick makes application of the FDM possible. The trick utilizes the fact that the right vertical boundary of Ω lies at $K\to\infty$. Thus, based on the asymptotic formula Equation (38), in this limit $\mathfrak{S}\to\infty$ as well, regardless of the value of $Z\in[0,SQ_T/D_T]$. Therefore, without any loss of accuracy, the domain Ω could be replaced with the domain $\tilde{\Omega}$ depicted in Exhibit 3.

By construction, the domain $\tilde{\Omega}$ is a parallelogram, and $K\in[0,K_{\max}]$, where $K_{\max}$ is some fixed strike. We introduce it to truncate an infinite strip in K to some fixed computational area.

Now, the parallelogram could be transformed to rectangle by using, e.g., the following affine transformation (for introduction to this topic see, e.g., Katsumi and Sasaki (1994)

EXHIBIT 3

The Domain $\tilde{\Omega}$: $\{K \in [0,\infty), Z \in [0, SQ_T]$

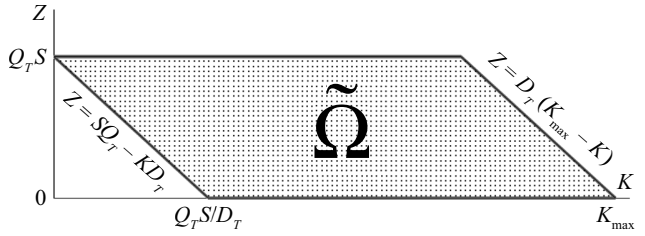

$$Z \mapsto SQ_T u, \qquad K \mapsto \frac{SQ_T}{D_T}(1-u) + \left(K_{\max} - \frac{SQ_T}{D_T}\right) v. \tag{56}$$

This transformation converts the domain $\tilde{\Omega}$ into a unit square, with the following map of the boundaries

$$\begin{aligned} &Z = SQ_T - KD_T \mapsto v = 0, \\ &Z = D_T(K_{\max} - K) \mapsto v = 1, \\ &Z = SQ_T \mapsto u = 1, \\ &Z = 0 \mapsto u = 0. \end{aligned} \tag{57}$$

Accordingly, we need to rewrite the operator $\mathcal{L}(T, K, Z)$ in new variables (u, v). For instance, for the parabolic operator Equation (48), this yields

$$\begin{aligned} \mathcal{L}(T,v,u) = &\frac{1}{2T}\mathfrak{S}^2 K_1^2[\mathfrak{S}_u^2 \partial_v^2 - 2\mathfrak{S}_u\mathfrak{S}_v \partial_u\partial_v + \mathfrak{S}_v^2 \partial_u^2] \\ &-[(r-q)v + B]\partial_v + qu\,\partial_u + \frac{1}{2T}, \\ B = &\frac{Q_T S(r(1-u)-q)}{D_T K_{\max} - SQ_T}, \end{aligned} \tag{58}$$

$$K_1 = \frac{c_1(1-u) + av}{a\mathfrak{S}_u + c_1\mathfrak{S}_v}, a = \frac{1}{SQ_T}, c_1 = \frac{1}{D_T K_{\max} - SQ_T}, \tag{59}$$

Since $\tilde{\Omega}$—the domain of definition of the operator $\mathcal{L}(T, v, u)$ in Equation (58)—is a unit square, now the PDE can be solved by using a FD method.

Splitting in Spatial Dimensions

Since computation of matrix exponent is time-consuming, especially in case of a two-dimensional operator L, we proceed with using a splitting technique, see Lanser and Verwer (1999); Duffy (2006); Itkin (2017b), and references therein. For instance, in Itkin (2017a), an ADI (alternative direction implicit) scheme proposed in In't Hout and Welfert (2007) for the solution of a backward PDE was extended twofold. First, a similar ADI scheme has been proposed for the forward equation, which equalizes the results obtained by solving backward and forward PDEs. Second, it replaces the first explicit step of the ADI, applied to the mixed derivative term of the PDE, with the fully implicit step. This is especially important for the forward PDE, as it increases the stability of the solution and guarantees its positivity.

However, for the PDE in Equation (55), using this ADI approach is not a trivial problem, mainly because of various problems with a stable approximation of the mixed derivative term at the second sweep of the ADI. Therefore, instead of the ADI method, here we use the Strang splitting, Lanser and Verwer (1999); Duffy (2006); Itkin (2017b). The main idea of this approach is as follows.

With allowance for Equation (58), let us represent the Equation (55) in the new coordinates in the form

$$\begin{aligned} \mathfrak{S}_T^{(k)} &= \left[\tilde{\mathcal{L}}_u^{(k-1)} + \tilde{\mathcal{L}}_v^{(k-1)} + \tilde{\mathcal{L}}_{uv}^{(k-1)}\right]\mathfrak{S}^{(k-1)}, \\ \mathcal{L}_u &= \frac{1}{2T}\mathfrak{S}^2 K_1^2 \mathfrak{S}_v^2 \partial_u^2 + qu\,\partial_u + \frac{1}{4T}, \\ \mathcal{L}_v &= \frac{1}{2T}\mathfrak{S}^2 K_1^2 \mathfrak{S}_u^2 \partial_v^2 - [(r-q)v + B]\partial_v + \frac{1}{4T}, \\ \mathcal{L}_{uv} &= -\frac{1}{T}\ \mathfrak{S}^2 K_1^2\ \mathfrak{S}_u\ \mathfrak{S}_v\ \partial_u\ \partial_v. \end{aligned} \tag{60}$$

Thus, the operator $\mathcal{L}_u$ includes all differentials with respect to u and also a half of the killing term in Equation (58). This is a linear convection-diffusion operator with state and time dependent coefficients. The operator $\mathcal{L}_v$ includes all differentials with respect to v and a half of the killing term in Equation (58), and also is a linear convection-diffusion operator with state and time dependent coefficients. Finally, the operator $\mathcal{L}_{uv}$ includes only a mixed derivatives term in Equation (58), and is also a linear diffusion operator with state and time dependent coefficients.

Equation (60) can be solved numerically by using the Strang splitting scheme

$$\begin{aligned} \mathfrak{S}^{(k)}(T+\Delta T,u,v) = &e^{\frac{\Delta T}{2}\tilde{\mathcal{L}}_u^{(k-1)}} e^{\frac{\Delta T}{2}\tilde{\mathcal{L}}_v^{(k-1)}} e^{\Delta T\tilde{\mathcal{L}}_{uv}^{(k-1)}} e^{\frac{\Delta T}{2}\tilde{\mathcal{L}}_v^{(k-1)}} e^{\frac{\Delta T}{2}\tilde{\mathcal{L}}_u^{(k-1)}} \\ &\mathfrak{S}^{(k-1)}(T+\Delta T,u,v) + O((\Delta T)^2). \end{aligned} \tag{61}$$

This scheme can also be represented as a sequence of *fractional* steps, which read

$$\begin{aligned}
\mathfrak{S}_1^{(k)} &= e^{\frac{\Delta T}{2}\tilde{\mathcal{L}}_u^{(k-1)}}\mathfrak{S}^{(k-1)},\\
\mathfrak{S}_2^{(k)} &= e^{\frac{\Delta T}{2}\tilde{\mathcal{L}}_v^{(k-1)}}\mathfrak{S}_1^{(k)},\\
\mathfrak{S}_3^{(k)} &= e^{\Delta T\tilde{\mathcal{L}}_{uv}^{(k-1)}}\mathfrak{S}_2^{(k)},\\
\mathfrak{S}_4^{(k)} &= e^{\frac{\Delta T}{2}\tilde{\mathcal{L}}_v^{(k-1)}}\mathfrak{S}_3^{(k)},\\
\mathfrak{S}^{(k)} &= e^{\frac{\Delta T}{2}\tilde{\mathcal{L}}_u^{(k-1)}}\mathfrak{S}_4^{(k-1)}.
\end{aligned} \tag{62}$$

We underline that the Strang splitting provides the second order approximation in ΔT only if the PDE at every fractional step in Equation (62) is solved also with the second order approximation in ΔT. To achieve that at every fractional step, we use the Padé approximation (1, 1) to obtain a Crank-Nicholson scheme in time. For instance, for the first line in Equation (62) it gives the following scheme

$$\left(1-\frac{1}{4}\Delta T\tilde{\mathcal{L}}_u^{(k-1)}\right)\mathfrak{S}_1^{(k)} = \left(1+\frac{1}{4}\Delta T\tilde{\mathcal{L}}_u^{(k-1)}\right)\mathfrak{S}^{(k-1)}. \tag{63}$$

Spatial Discretization

To apply this algorithm, we construct an appropriate discrete non-uniform grid $\mathbf{G}(x)$ in the (u, v) space, see Itkin (2017b). In each spatial direction $i \in [u, v]$, a non-uniform grid contains $N_i + 1$ nodes $(p_0, p_1, ..., p_{Ni})$, with the steps $h_1 = p_1 - p_0, ..., h_{Ni} = p_{Ni} - p_{Ni-1}$. Accordingly, in the operator Equation (58), we replace continuous derivatives with their finite-difference approximations, and denote these discrete operators defined on $\mathbf{G}(x)$ as ∇. Thus, we replace ∂_x with ∇_x, etc.

Approximation of derivatives. Once a non-uniform grid is constructed, the first and second derivatives can be approximated on this grid. The corresponding expressions are obtained by using the Taylor series expansions. Here for reference we just provide the final results, see, e.g., Itkin (2017b); In't Hout and Foulon (2010):

Let f: $\mathbb{R} \to \mathbb{R}$ be any given function, let x_i, $i \in \mathbb{Z}$ be any given increasing sequence of mesh points, and $h_i = x_i - x_{i-1}$, $\forall i$. To approximate the first derivatives of $f(x)$, employ the following formulas.

Backward scheme:

$$\begin{aligned}
\nabla_x^{1B} &= \alpha_{-2}f(x_{i-2}) + \alpha_{-1}f(x_{i-1}) + \alpha_0 f(x_i)\\
&= f'(x_i) + O((h_i + h_{i-1})^2),
\end{aligned}$$

Forward scheme:

$$\begin{aligned}
\nabla_x^{1F} &= \gamma_0 f(x_i) + \gamma_1 f(x_{i+1}) + \gamma_2 f(x_{i+2})\\
&= f'(x_i) + O((h_{i+1} + h_{i+2})^2).
\end{aligned}$$

Central scheme:

$$\begin{aligned}
\nabla_x^{1C} &= \beta_{-1}f(x_{i-1}) + \beta_0 f(x_i) + \beta_1 f(x_{i+1})\\
&= f'(x_i) + O((h_i + h_{i+1})^2).
\end{aligned} \tag{64}$$

Here the super index ^{1X} means the first derivatives with the X approximation, $X \in [B, F, C]$ could be backward (B), forward (F), and central (C), and the coefficients α, β, γ read

$$\begin{aligned}
\alpha_{-2} &= \frac{h_i}{h_{i-1}(h_i + h_{i-1})}, \alpha_{-1} = -\frac{h_{i-1} + h_i}{h_i h_{i-1}},\\
\alpha_0 &= \frac{h_{i-1} + 2h_i}{h_i(h_{i-1} + h_i)},\\
\gamma_0 &= -\frac{2h_{i+1} + h_{i+1}}{h_{i+2}(h_{i+2} + h_{i+1})}, \gamma_1 = \frac{h_{i+2} + h_{i+1}}{h_{i+2}h_{i+1}},\\
\gamma_2 &= -\frac{h_{i+1}}{h_{i+2}(h_{i+2} + h_{i+1})}.\\
\beta_{-1} &= -\frac{h_{i+1}}{h_i(h_{i+1} + h_i)}, \beta_0 = \frac{h_{i+1} - h_i}{h_{i+1}h_i},\\
\beta_1 &= \frac{h_i}{h_{i+1}(h_{i+1} + h_i)}.
\end{aligned}$$

As follows from Equation (64), these expressions provide approximation of the first derivatives with the second order $O(h^2)$.

To approximate the second derivatives of $f(x)$, one can employ the following formulas.

$$\nabla_x^{2C} = \nabla_x^{1F}\nabla_x^{1B} = \nabla_x^{1B}\nabla_x^{1F}, \quad \nabla_x^{2B} = \nabla_x^{1B}\nabla_x^{1B}, \quad \nabla_x^{2F} = \nabla_x^{1F}\nabla_x^{1i}$$

These expressions provide approximation of the second derivatives also with the second order $O(h^2)$. For instance, for ∇_x^{2C} we have in the explicit form

$$\begin{aligned}
\nabla_x^{2C} &= \delta_{-1}f(x_{i-1}) + \delta_0 f(x_i) + \delta_1 f(x_{i+1})\\
&= f''(x_i) + O((h_i + h_{i+1})^2),
\end{aligned}$$

where

$$\delta_{-1} = \frac{2}{h_i(h_{i+1}+h_i)}, \quad \delta_0 = -\frac{2}{h_{i+1}h_i}, \quad \delta_1 = \frac{2}{h_{i+1}(h_{i+1}+h_i)}.$$

Let f: $\mathbb{R}^2 \to \mathbb{R}^2$ be any given function of two variables (x, y). To approximate the mixed derivative $\partial_{x,y} f(x_i, y_j)$ at any point (x_i, y_j), one can consequently apply either one-sided approximations in each direction, or apply the central difference approximation first in x and then in y (or vice versa). The latter results in the FD approximation of the mixed derivative using a 9-point stencil while still providing the second order of approximation. However, as shown in Itkin (2017a), this discretization could be unstable. Therefore, a fully implicit scheme was proposed instead that, as applied to our problem, is discussed in the next section.

For the future, we need some additional notation. We denote a matrix of ∇_x^{1F} as $A_{1,x}^{2F}$; the matrix of ∇_x^{1B}—as $A_{1,x}^{2B}$; the matrix of ∇_x^{1C}—as $A_{1,x}^{2C}$.[2] For the first order approximations, we use the following definitions. Define a one-sided *forward* discretization of ∇, which we denote as $A_{1,x}^{1F} : A_{1,x}^{1F} C(x) = [C(x+h,t) - C(x,t)]/h$. Also define a one-sided *backward* discretization of ∇, denoted as $A_{1,x}^{1B} : A_{1,x}^{1B} C(x) = [C(x,t) - C(x-h,t)]/h$. These discretizations provide first order approximation in h, e.g., $\partial_x C(x) = A_{1,x}^{1F} C(x) + O(h)$. Also I_x denotes a unit matrix.

Approximation of the operator $\mathcal{L}(T, v, u)$. Here we use the same approach as in Itkin (2018). Denote $A_{2,x}^{2C}$ a matrix of the discrete operator ∇_x^{2C} on the grid $\mathbf{G}(x)$. Observe, that $A_{2,x}^{2C}$ is the Metzler matrix, see Berman and Plemmons (1994); Itkin (2017b). Indeed, it has all negative elements on the main diagonal, and all non-negative elements outside of the main diagonal. Also $A_{2,x}^{2C}$ is a tridiagonal matrix.

By the properties of the Metzler matrix M, its exponent is a nonnegative matrix. Therefore, operation $e^{\mathcal{M}}\mathfrak{S}$ preserves positivity of vector $\mathfrak{S}$. Also, all eigenvalues of the Metzler matrix have a negative real part. Therefore, the spectral norm of the matrix follows

$$\| e^M \| < 1.$$

Thus, if in Equation (54) the operator $\mathcal{M} = \tilde{\mathcal{L}}^{(k-1)}$ on the grid $\mathbf{G}(x)$ is represented by the Metzler matrix $A_{\mathcal{M}}$, the map $e^{A_{\mathcal{M}}}$ is contractual, and, hence, the entire scheme Equation (54) is stable.

By the definition of the operator $\tilde{\mathcal{L}}^{(k-1)}$ in Equation (60), it consists of several terms.

Second derivatives. The first term $\frac{1}{2T}\mathfrak{S}^2 K_1^2 \mathfrak{S}_u^2 \partial_v^2$ can be approximated on the grid as

$$A_{2,v} = \frac{1}{2T}\mathfrak{S}^2 K_1^2 \mathfrak{S}_u^2 A_{2,v}^{2C}.$$

As $T > 0$, obviously $A_{2,v}$ is the Metzler matrix. The same is true for the matrix $A_{2,u}$:

$$A_{2,u} = \frac{1}{2T}\mathfrak{S}^2 K_1^2 \mathfrak{S}_v^2 A_{2,u}^{2C}.$$

The mixed derivative. The mixed derivative term in Equation (60) reads: $-\frac{1}{T}\mathfrak{S}^2 K_1^2 \mathfrak{S}_u \mathfrak{S}_v \partial_u \partial_v$. Observe, that from Equation (56) we have

$$\mathfrak{S}_u = \frac{SQ_T}{D_T}(D_T \mathfrak{S}_Z - \mathfrak{S}_K), \qquad \mathfrak{S}_v = \mathfrak{S}_K \left(K_{\max} - \frac{SQ_T}{D_T} \right),$$

from Equation (25)

$$\mathfrak{S}_Z = \frac{\sqrt{T}}{BS_\sigma(K, \Sigma, T)} \geq 0,$$

and from Equation (29), Equation (31)

$$\mathfrak{S}_K = -\mathfrak{S}_Z BS_K(S, \Sigma, T) = \mathfrak{S}_Z D_T N(d_2(K, \Sigma, T)) \geq 0.$$

With the allowance for these expressions, it follows that

$$\begin{aligned}
\mathfrak{S}_u &= \frac{\sqrt{T}}{BS_\sigma(K, \Sigma, T)} SQ_T \left[1 - N(d_2(K, \Sigma, T))\right] = sR(d_2) \geq 0, \\
\mathfrak{S}_v &= \frac{\sqrt{T}}{BS_\sigma(K, \Sigma, T)} N(d_2(K, \Sigma, T))(D_T K_{\max} - SQ_T) \\
&= \left(\frac{K_{\max}}{K} - s \right) \left(\sqrt{2\pi} e^{d_2^2/2} - R(d_2) \right) \geq 0, \\
s &= \frac{SQ_T}{KD_T}, \qquad d_2 = d_2(K, \Sigma, T),
\end{aligned} \tag{65}$$

where $R(x) \equiv \frac{1 - N(x)}{N'(x)}$ is the Mills ratio for the standard normal distribution. It can be efficiently computed by

[2] Hence, e.g., for $A_{1,x}^{2F}$, the superscript means: backward second order approximation, and subscript means: first order derivative.

the particularly simple continued fraction representation at $x > 1$

$$R(x) = \cfrac{1}{x + \cfrac{1}{x + \cfrac{2}{x + \ldots}}}, \tag{66}$$

or by using Taylor series expansion at $0 \le x \le 1$, see Gasull and Utzet (2013).

Thus, $\mathfrak{S}_u \mathfrak{S}_v \ge 0$. Therefore, to have $A_{2,uv}$ to be the Metzler matrix, we need the matrix of $\mathfrak{S}_u \mathfrak{S}_v$ to be the negative of the Metzler matrix[3], again see Itkin (2017b). However, the standard methods fail to provide discretization of the second order that guarantees this feature. Therefore, we need another approach, similar to what was proposed in Itkin (2017a). We discuss this in Appendix A.

As compared with Itkin (2017a), the method in this article has two innovations. First, in Itkin (2017a), a first order approximation in time step was constructed, while here we provide the second order approximation. Second, in Itkin (2017a), a mixed derivative term has the form $\rho_{u,v} f(v) g(u) \partial_u \partial_v$, where $f(u)$ is some function of u only, and $g(v)$ is some function of v only. Here we deal with a more general term $\rho_{u,v} f(u,v) \partial_u \partial_v$, and show that the approach of Itkin (2017a) can be applied in this case as well.

Convection terms. The next step is to construct a suitable approximation for the convection terms. The term $qu\partial_u$ admits the forward approximation ∇_u^{1F} as $q \ge 0$ and $u \in [0,1]$. Approximating the term $-[(r-q)v + B]\,\partial_v$ is a more delicate issue and depends on the sign of the function $F(u,v) = (r-q)v + B$. Suppose $r > q$. A typical behavior of function $F(u,v)$ at $T = 0.01$ is presented in Exhibit 4 at the values of model parameters given in Exhibit 1.

As can be seen, $F(u,v) \ge 0$ for all values of $(u,v) \in [0,1] \times [0,1]$. Therefore, when approximating the term $-F(u,v)\partial_v$. a *backward* approximation should be used to obtain the Metzler matrix, i.e., $-F(u,v)A_{2,v}^{1B}$. It can be checked that in case $r < q$, the *forward* approximation should be used as then $F(u,v) \le 0$.

[3] Rigorously speaking, the matrix $A_{2,uv}$ should be the negative of the EM-matrix, where the latter stays for the Eventually M-Matrix. For the introduction into the EM matrices and their properties see Itkin (2017b).

EXHIBIT 4

The Behavior of Function $F(u, v)$ at $T = 0.5$

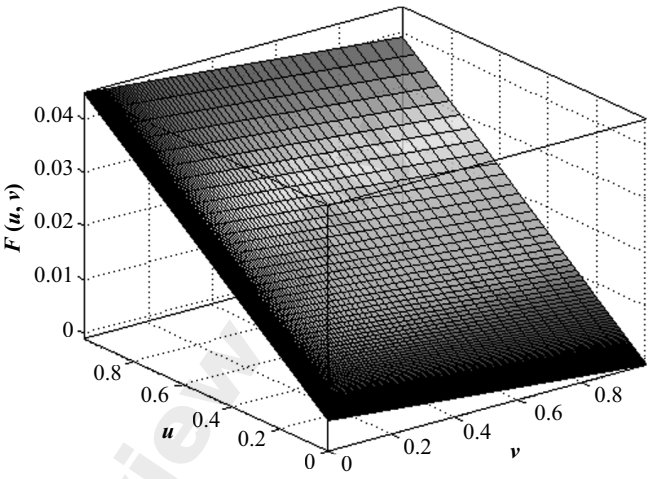

Finally, the resulting matrices $A_{\tilde{\mathcal{L}}_u}$, $A_{\tilde{\mathcal{L}}_v}$, are, by construction, also the Metzler matrices, as each of them is a sum of the Metzler matrices, Berman and Plemmons (1994).

It is easy to prove that the matrix $\exp(A_{\tilde{\mathcal{L}}^{(k-1)}})$ is the second order approximation of the operator $e^{\mathcal{M}}$ in the spatial steps h_u, h_v on the grid, i.e., $O(h_u^2 + h_v^2 + h_u h_v)$. That follows from the fact that the derivatives are approximated by using Equation (64), where every line is the second order approximation to the corresponding partial derivative.

Convergence of Picard Iterations

The remaining point to prove is the convergence of the fixed-point Picard iterations. Again, in doing so, we follow Itkin (2018). According to Equation (54), change of variables in Equation (56), and Equation (55) we run the iterations

$$\mathfrak{S}^{(k)}(T + \Delta T, u, v) = e^{\Delta T \tilde{\mathcal{L}}^{(k-1)}}\, \mathfrak{S}^{(k-1)}(T, u, v), \quad k > 1. \tag{67}$$

By construction, at every iteration k the operator $\tilde{\mathcal{L}}^{(k)}$ is linear, continuous, and bounded at the computational domain. Also, the operator $\varepsilon = \exp[\Delta T \tilde{\mathcal{L}}^{(k)}]$ is Lipschitz

$$\|\varepsilon \mathfrak{S}_1(T,u,v) - \varepsilon \mathfrak{S}_2(T,u,v)\| \le \|\varepsilon\| \|\mathfrak{S}_1(T,u,v) - \mathfrak{S}_2(T,u,v)\|,$$

EXHIBIT 5
Parameters of the Test

S	r	q	$T_{\max}$	$K_{\max}$	Call/Put	N_u	N_v	R_c
100.00	0.05	0.01	1.00	400.00	Call	200	100	20

since we constructed discretization of ε as e^M with M being the Metzler matrix, and it was shown earlier that in the spectral norm $\|e^{\mathcal{M}}\| \le 1$.

Now, to prove convergence of the Picard iterations denote by $\hat{\mathfrak{S}}(T+\Delta T,u,v)$ the exact solution of Equation (47) at time $T+\Delta T$. Then, by the mean-value theorem for operators, we have

$$\|\mathfrak{S}^{(k)}(T+\Delta T,u,v)-\hat{\mathfrak{S}}(T+\Delta T,u,v)\|=\|\varepsilon\mathfrak{S}(T,u,v)$$
$$-\hat{\varepsilon}I\mathfrak{S}(T,u,v)\|\le\|\mathbb{D}(\varepsilon)(\xi^{(k)})\|\cdot\|\mathfrak{S}^{(k-1)}(T+\Delta T,u,v)-\hat{\mathfrak{S}}(T,u,v)\|$$

where $\xi^{(k)}$ is a convex combination of $\mathfrak{S}^{(k-1)}(T+\Delta T,u,v)$ and $\mathfrak{S}^{(k)}(T+\Delta T,u,v)$, and $\mathbb{D}$ denotes the Frèchet derivative of the operator ε at the space of all bounded nonlinear operators, see, e.g., Hutson, Pym, and Cloud (2005) and Li et al. (2010). Thus, the iterations converge if $\|\mathbb{D}(\varepsilon)\| < 1$. We prove that actually this is the case for the operators in Equation (60) in Appendix B. In particular, we show there that the iterative scheme is "almost" unconditionally stable, where "almost" means for the values of the model parameters that are reasonable from a practical point of view.

All the results obtained in this section can be further summarized in the following proposition

Proposition 6.1. *The scheme Equation (54) with approximation Equation (67) is a) (almost) unconditionally stable, b) preserves non-negativity of the solution, c) provides second order approximation of Equation (54) in space on the grid, and d) converges.*

NUMERICAL RESULTS AND COMPARISON

In our numerical test we use the input parameters shown in Exhibit 5. We build a non-uniform grid $\mathbf{G}(x)$ in the (u,v) space, which contains N_u nodes in the u direction and N_v nodes in the v direction. Since the gradients of the implied volatility $\mathfrak{S}(T,u,v)$ are high at the boundaries of the computational domain, i.e., close to $u=0$, 1 and $v=0$, 1 it makes sense to make the grid denser close to these areas. Since from practical purposes the far boundary is of a less interest, we compress the grid close to the lines $u=0$, $v=0$. This is obtained by using the compression ratio $R_c=50$, see the description in Itkin (2017b). Thus constructed grid is represented in Exhibit 6. With the initial parameters in Exhibit 5, one step in the v direction approximately corresponds to a change in strike by 3$, and one step in the u direction approximately corresponds to a 50 cents change in both the options price and the strike.

EXHIBIT 6
Non-Uniform Finite-Difference Grid in *(u, v)* Space

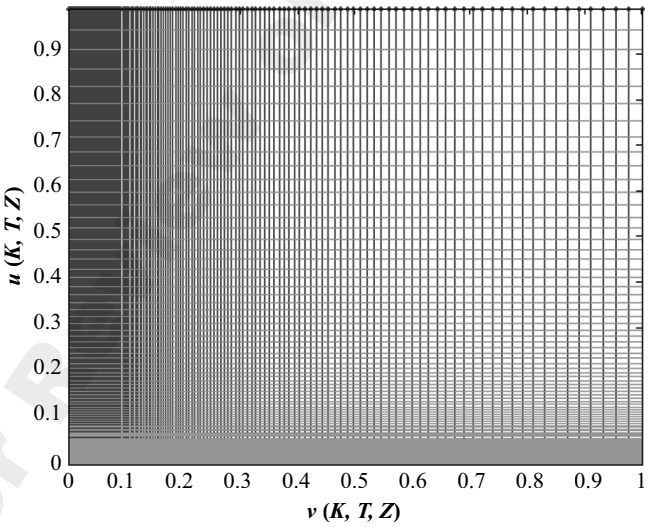

We solve the forward equation starting at $T=0$ and going forward in time to $T_{\max}$, with the time step $\Delta T=0.01$. The boundary conditions are computed, as this is described previously using the numerical solutions of Equation (36), Equation (39), and Equation (40). Thus, the found boundary values corresponding to $T=0.01$ are presented in Exhibit 7 (along the lines $u=0$, $u=1$, $v=0$ and $v=1$).

The standard way to get the implied volatility by solving Equation (2) numerically is used for comparison, and further is called "traditional." We run this

EXHIBIT 7

Implied Volatility $\mathfrak{S}(K,Z,T)$ at $T = 0.01$ Computed by Using the Traditional Approach

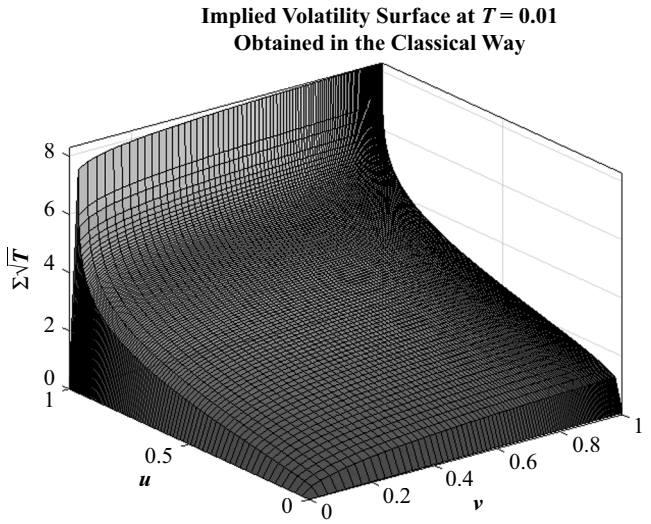

EXHIBIT 8

Implied Volatility $\mathfrak{S}(K,Z,T)$ at $T = 0.5$ Computed by Using the Traditional Approach (zoomed-in)

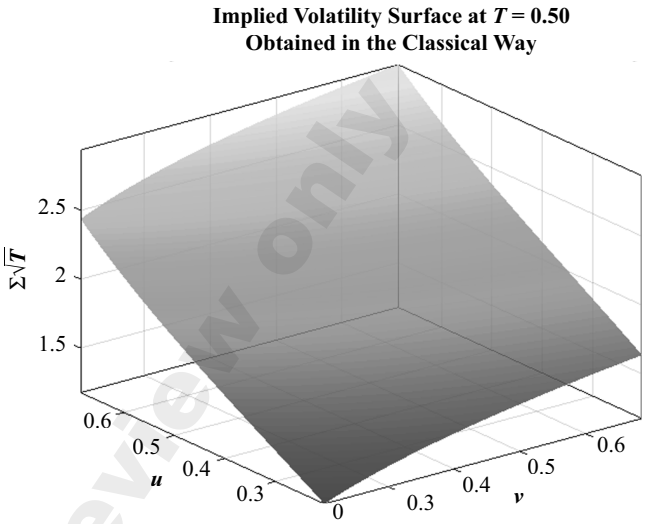

traditional approach at every point of the grid $\mathbf{G}(x)$ by using Matlab function blsimpv, or a root solver at the boundaries where blsimpv provides unsatisfactory results. All tests were run on a PC with Intel i7-4790 CPU (8 Cores, 3.6GHz) as a sequential loop, i.e., no parallel tools have been used. The total elapsed time was 113 secs for 20,000 points on the grid, or, on average, 6 msc per a single point.. The results are presented in Exhibit 7.

The grid $\mathbf{G}(x)$ doesn't change in time. On the other hand, functions $d_1(\mathfrak{S})$, $d_2(\mathfrak{S})$ in the Black-Scholes formula (see Equation (19)) also almost don't depend on T (since T is now embedded into $\mathfrak{S}$). Therefore, the only dependence on T in the numerical implementation of Equation (2) is the dependence of Q_T, D_T, which is weak. Thus, Exhibit 7 changes with time very slowly. Also, for the purpose of a better illustration of the behavior of $\mathfrak{S}$ at intermediate values of (u, v), we zoom-in to Exhibit 7 by excluding the boundaries and setting $T = 0.5$. Thus obtained plot is represented in Exhibit 8.

First Step in Time

The first step in time is the most challenging problem with our approach. Indeed, the initial condition for the PDE in Equation (55) is $\mathfrak{S}(0,u,v) = 0$ for all u and v. This, in turn, means that all gradients $\mathfrak{S}_u$, $\mathfrak{S}_v$ tend to infinity at $T = 0$. Also,

$$\tilde{\mathcal{L}}^{NL}(0,u,v) = 0, \tag{68}$$

where $\mathcal{L}^{\text{NL}}$ denotes the nonlinear part of the operator $\mathcal{L}$. Therefore, the iterative scheme in Equation (55) becomes incorrect. At the moment we don't have a good resolution of this problem. Therefore, instead, for $T = \Delta T$ we proceed by computing $\mathfrak{S}(\Delta T,u,v)$ in the traditional way, and denote the obtained implied volatility as $\mathfrak{S}_{tr}(\Delta T,u,v)$.

Again, the main problem here is that at $T = \Delta T$ we don't have a good initial guess for $\mathfrak{S}$, as it cannot be taken from the previous time step. But, in principle, if we would have a good initial guess for $\mathfrak{S}$, we could run our iterative algorithm even at $T = \Delta T$. To validate this, we further use $\mathfrak{S}_{tr}(\Delta T,u,v)$ as the initial guess for the iterative scheme. But, based on Equation (68), for this time step we also need to modify the scheme in Equation (55) to be

$$\mathfrak{S}_T^{(k)} = \mathcal{L}^{(k-1)}(T+\Delta T,K,Z)\,\mathfrak{S}^{(k-1)} = \tilde{\mathcal{L}}^{(k-1)}\,\mathfrak{S}^{(k-1)}. \tag{69}$$

Then we solve this equation iteratively, but it is easy to check that this scheme provides only the first order approximation in ΔT.

EXHIBIT 9

The Difference $\Delta\mathfrak{S} = \mathfrak{S}_{tr}(\Delta T, u, v) - \mathfrak{S}(\Delta T, u, v)$ as a Function of u, v at $T = 0.01$ after 20 Iterations

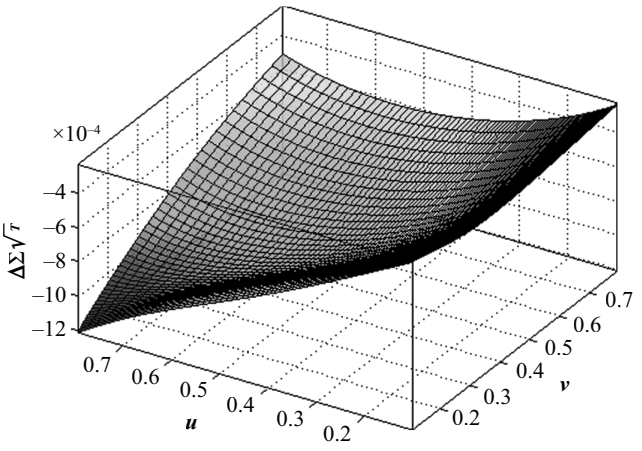

The results are as follows. We do 20 iterations of the method to obtain the relative error

$$\varepsilon = \frac{\|\mathfrak{S}_{tr}(\Delta T, u, v) - \mathfrak{S}(\Delta T, u, v)\|}{\|\mathfrak{S}_{tr}(\Delta T, u, v)\|}$$

to be 1.5 bps. The elapsed time for doing so is 16 secs, or 0.8 secs per iteration. The difference between $\mathfrak{S}_{tr}(\Delta T, u, v)$ and our numerical solution $\mathfrak{S}(\Delta T, u, v)$ is presented in Exhibit 9. The graph is truncated up to $u = v = 0.8$ because very large values of strikes don't have practical interest.

Next Steps in Time

Having good (not all zeros) values of $S(\Delta T, u, v)$ we can proceed based on the general scheme described in earlier. We increase time to $T = 2\Delta T$, iterate to get the numerical solution, then compute $S_{tr}(2\Delta T, u, v)$, compare these solutions, etc. In Exhibit 10, these results are presented for $T = 2\Delta T$, $5\Delta T$, $10\Delta T$, and $20\Delta T$.

It turns out that at those time steps, the iterations converge much faster, as compared with the test for the first step reported in the previous section. This convergence is summarized in Exhibit 11. This partially could be explained by the order of approximation in time, since at the first step the scheme was of the order one, while at the next steps it is of the order two.

As this can be seen from the presented results, the convergence of the method slightly improves with time T, the elapsed time remains the same, while the relative error between the traditional method and the PDE solver slightly increases with T. The latter can obviously be explained by accumulation of the approximation errors at every time step with the increase of T. However, for instance, for $T = 0.2$, this error is still acceptable (to be 20–50 bps). On the other hand, the biggest deviation from the traditional results corresponds to high u and v. In particular, in our numerical example, the point $u = v = 0.8$ maps to the strike $K = 260\$$ which, in turn, corresponds to the moneyness $S/M = 0.385$ and the option price 20$. Hence, this is a deep OTM option, and the corresponding implied volatility is very high, 2.61. Therefore, this case is almost impractical.

DISCUSSION

In this article, we derive backward and forward quasilinear parabolic PDEs that govern the implied volatility of a contingent claim whenever the latter is well-defined. This would include at least any contingent claim written on a positive stock price whose payoff at a possibly random time is convex. Alternatively, we derive a forward nonlinear hyperbolic PDE of the first order, which also governs the evolution of the implied volatility in (K, T, Z) space. We discuss suitable initial and boundary conditions for those PDEs. Finally, we demonstrate how to solve them numerically by using an iterative method. All of these results are new.

We compare performance of two methods. The first one uses a traditional scheme of getting the implied volatilities by using a root solver and solving Equation (2). The second method relies on a numerical solution of the derived PDEs. We show that based on our numerical experiments, if the implied volatility is needed at every point on the rather dense grid, the PDE solver significantly outperforms the root solver. As follows from Exhibit 11, the PDE solver is almost 40 times faster.[4]

However, a few comments should be made in this regard. First, our method utilizes the traditional method

[4] As mentioned previously, the total elapsed time for the traditional solver in this test is 113 secs. And the same time for the PDE solver, as reported in Exhibit 11, is 2.8 secs. Therefore, the ratio is about 40.

EXHIBIT 10

The Difference $\Delta\mathfrak{S} = \mathfrak{S}_{tr}(\Delta T, u, v) - \mathfrak{S}(\Delta T, u, v)$ as a Function of u, v at $T = 0.02$ (upper-left), $T = 0.05$ (upper-right), $T = 0.1$ (bottom-left), and $T = 0.2$ (bottom-right)

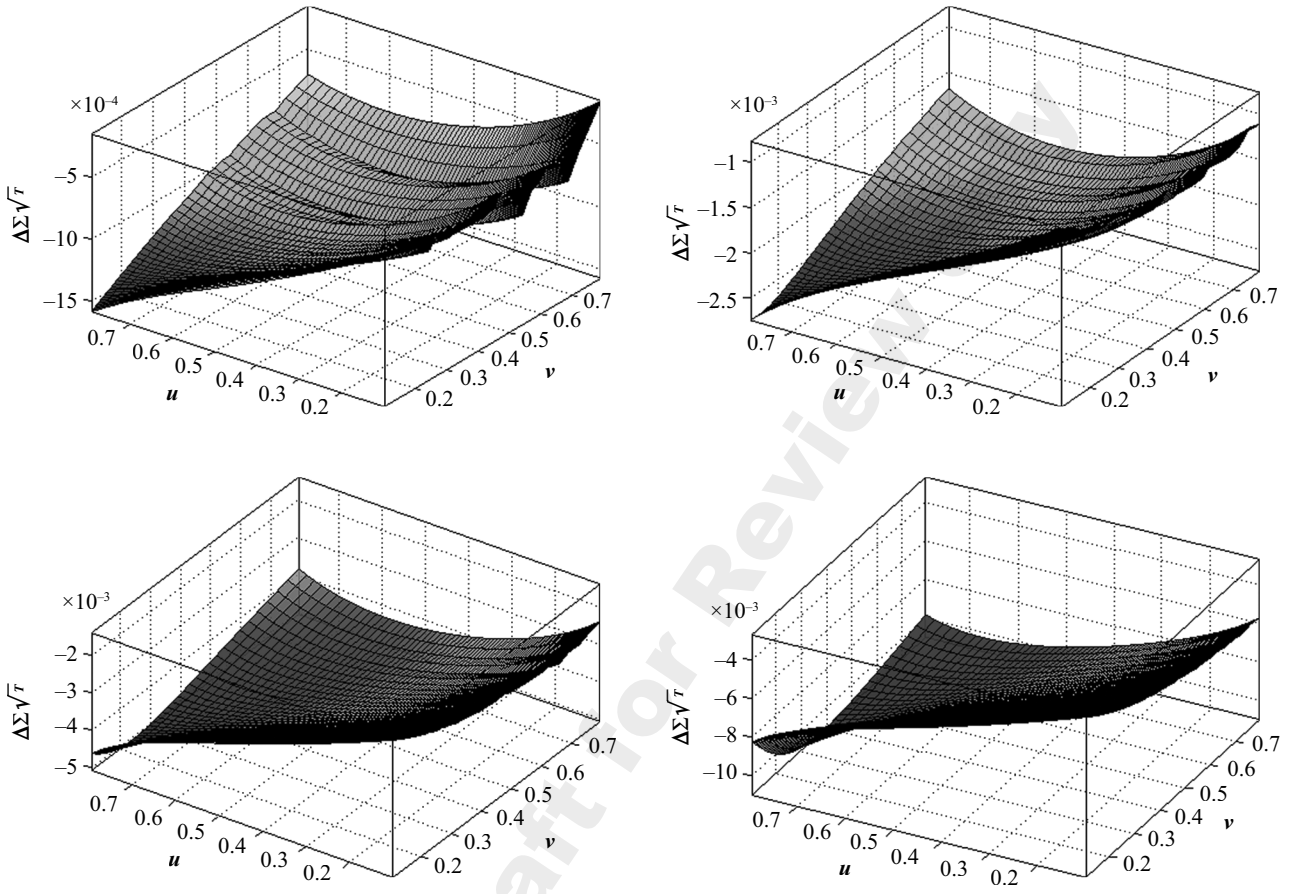

in two ways. We use it to compute the boundary conditions, and we also use it at the first time step $T = \Delta T$ since we don't have a good start value of $\mathfrak{S}$ for iterations to kick off. Also, this drops the order of approximation in time from $O((\Delta T)^2)$ to $O(\Delta T)$ at this step. Nevertheless, all of those issues are relatively minor, and for the longer time horizons, our method still outperforms the traditional one.

The second obstacle is that, most likely, in practice we rarely need implied volatilities on such a dense grid in both space and time. Usually, we need them only at those points in (K, T), which correspond to the tradable market strikes and maturities, and they are not so dense. However, the FD method still requires a grid. Therefore, the number of points for the traditional method could be much smaller than that for the FD method. This could compensate for the slower performance of the traditional method and make both methods comparable in the elapsed time.

Third, the functions $d_1(\mathfrak{S})$, $d_2(\mathfrak{S})$ in the Black-Scholes formula (see Equation (19)) weakly depend on T (since T is now embedded into $\mathfrak{S}$), namely only via Q_T and D_T. Therefore, the solution of Equation (2) also depends on T only via Q_T, D_T. Therefore, since we already computed $\mathfrak{S}(\Delta T, K, Z)$ by using the traditional way, then for $T = 2\Delta T$ Equation (2) could be solved by expanding the left hand side into a series on $\Delta T \ll 1$. In more detail, we write

$$B\mathfrak{S}(T, K, \mathfrak{S}(T, K, Z)) = Z,$$
$$B\mathfrak{S}(T + \Delta T, K, \mathfrak{S}(T + \Delta T, K, Z)) = Z, \qquad (70)$$

EXHIBIT 11

Convergence of the Picard Iterations for Various Steps in Time *T*. The Time Step $\Delta T = 0.01$

Step in Time	Iterations Per Step	ε	*t* Elapsed, Secs
1	20	1.5e-4	16
2	3	2.3e-6	2.7
3	3	1.9e-6	2.8
5	3	1.4e-6	2.8
10	3	8.3e-7	2.8
20	3	3.8e-7	2.8

and define $\mathfrak{S}(T+\Delta T,K,Z)=\mathfrak{S}(T,K,Z)+\Delta\mathfrak{S}(T,K,Z)$. Now expanding the second line of Equation (70) into series on $\Delta T \ll 1$, $\Delta\mathfrak{S} \ll 1$, and using the first line in Equation (70), in the first order we obtain

$$\Delta\mathfrak{S}(T,K,Z)=-\frac{\Theta(T,K,\mathfrak{S}(T,K,Z))}{\text{Vega}(T,K,\mathfrak{S}(T,K,Z))}\sqrt{T}\Delta T. \quad (71)$$

Since $\mathfrak{S}(T,K,Z)$ is already known, the expression in Equation (71) can be easily computed.

Once all $\mathfrak{S}(T+\Delta T,K,Z)$ are computed in such a way, we can proceed to $T+2\Delta T$. The problem with this approach, however, is that its accuracy decreases with every time step. As an alternative, periodically at some time steps, the accurate value of $\mathfrak{S}(T,K,Z)$ can be recomputed by using the traditional approach. However, same could be done for the PDE approach as well.

It should also be mentioned that in this article we present results for European plain vanilla options using the forward equation, while for American options, one has to solve the backward PDE, which computationally is more expensive.

APPENDIX A

FD APPROXIMATION OF THE MIXED DERIVATIVE TERM IN EQUATION (60)

In this Appendix, we show how to solve the third line in Equation (62) with the accuracy $O((\Delta T)^2)$ in time and $O(h_u^2+h_v^2+h_uh_v)$ in space following the method first proposed in Itkin (2017a). To recall, the equation under consideration reads

$$\mathfrak{S}^{(k)}=e^{\Delta T\tilde{\mathcal{L}}_{uv}^{(k-1)}}\mathfrak{S}^{(k)},$$
$$\mathcal{L}_{uv}=-\frac{1}{T}\mathfrak{S}^2K_1^2\,\mathfrak{S}_u\,\mathfrak{S}_v\nabla_u\nabla_v. \quad (A1)$$

To achieve this accuracy in time we use the Padé approximation (1, 1) to obtain a Crank-Nicholson scheme (written with some loss of notation to make it more readable)

$$\left(1-\frac{1}{4}\Delta T\tilde{\mathcal{L}}_{uv}^{(k-1)}\right)\mathfrak{S}(T+\Delta T)=\left(1+\frac{1}{4}\Delta T\tilde{\mathcal{L}}_{uv}^{(k-1)}\right)\mathfrak{S}(T)=\overline{\mathfrak{S}}(T). \quad (A2)$$

This numerical scheme is, of course, implicit due to the fact that, despite we know $\overline{\mathfrak{S}}(T)$, to find $\mathfrak{S}(T+\mathbb{D}T)$ we need to solve Equation (A2). It is known that, after some discretization on the FD grid is applied to Equation (A2), the matrix in the left hands side of Equation (A2) must be an M-matrix, to ensure that this scheme is stable and preserves the positivity of the solution. However, this is impossible by using the standard FD discretizations of the second order, in more detail see Itkin (2017b).

Therefore, we rewrite Equation (A2) by dropping the dependence on T and using a trick proposed in Itkin (2017a)[5]

$$\begin{aligned}&(P-\sqrt{\Delta T}\rho_{u,v}U(u,v)\nabla_u)(Q+\sqrt{\Delta T}V(u,v)\nabla_v)\mathfrak{S}\\&=\overline{\mathfrak{S}}+\left[(PQ-1)-Q\sqrt{\Delta T}\rho_{u,v}U(u,v)\nabla_u\right.\\&\quad\left.+P\sqrt{\Delta T}V(u,v)\nabla_v\right]\mathfrak{S}.\\&U(u,v)=\frac{1}{\sqrt{T}}\mathfrak{S}K_1\mathfrak{S}_u,\qquad V(u,v)=\frac{1}{\sqrt{T}}\mathfrak{S}K_1\mathfrak{S}_v. \quad (A3)\end{aligned}$$

Here $\rho_{u,v}=-1/4$,[6] P, Q, are some positive numbers that have to be chosen based on some conditions, e.g., to provide diagonal dominance of the matrices in the parentheses in the left hand side of Equation (A3), see below. Also the intuition behind this representation is discussed in detail in Itkin (2017a).

Note, that in Itkin (2017a), we considered a mixed derivative term of the form $\rho_{u,v}f(v)g(u)\partial_u\partial_v$, where $f(u)$ is some function of u only, and $g(v)$ is some function of v only. Here we are dealing with a more general term $\rho_{u,v}f(u,v)\partial_u\partial_v$, so the presented approach is a generalization of that in Itkin (2017a). Also, our method in this article is of the second order in time, while the method in Itkin (2017a) is of the first order.

[5] The trick is motivated by the desire to build an ADI scheme which consists of two one-dimensional steps, because for the 1D equations we know how to make the right hand side matrix to be an EM-matrix, see Itkin (2016); Itkin (2017b), and references therein.

[6] We introduce this notation to make it easy to compare the description of the method in this article with that in Itkin (2017a).

The Equation (A3) can be solved using fixed-point Picard iterations. One can start with setting $\mathfrak{S}^0 = \overline{\mathfrak{S}}$ in the right hands side of Equation (A3), then solve sequentially two systems of equations

$$\begin{aligned}&(Q+\sqrt{\Delta T}V(u,v)\nabla_v)\mathfrak{S}^* = \overline{\mathfrak{S}}+[PQ-1\\&\quad -Q\sqrt{\Delta T}\rho_{u,v}U(u,v)\nabla_u+P\sqrt{\Delta T}V(u,v)\nabla_v]\mathfrak{S}^j,\\&(P-\sqrt{\Delta T}\rho_{u,v}U(u,v)\nabla_u)\mathfrak{S}^{j+1} = \mathfrak{S}^*.\end{aligned} \tag{A4}$$

Here S^j is the value of S at the j-th iteration[7].

To solve Equation (A4), we propose two FD schemes. The first one (Scheme A) is introduced by the following Propositions[8]:

Proposition A.1. *Let us approximate the left hand side of Equation (A4) using the following finite-difference scheme:*

$$\begin{aligned}&(QI_v+\sqrt{\Delta T}V(u,v)A^{2B}_{1,v})\mathfrak{S}^* = \alpha^+\overline{\mathfrak{S}}-\mathfrak{S}^j,\\&(PI_u-\sqrt{\Delta T}\rho_{u,v}U(u,v)A^{2B}_{1,u})\mathfrak{S}^{j+1} = \mathfrak{S}^*,\\&\alpha^+ = (PQ+1)I-Q\sqrt{\Delta T}\rho_{u,v}U(u,v)A^{1F}_{1,u}+P\sqrt{\Delta T}V(u,v)A^{1F}_{1,v}.\end{aligned} \tag{A5}$$

Then this scheme is unconditionally stable in time step ΔT*, approximates Equation (A4) with* $O(\sqrt{\Delta T}\max(h_u,h_v))$*, and preserves positivity of the matrix* $\mathfrak{S}(u,v,T)$ *if* $Q=\beta\sqrt{\Delta T}/h_v$, $P=\beta\sqrt{\Delta T}/h_u$*, where* h_v, h_u *are the grid space steps correspondingly in* v *and* u *directions, and the coefficient* β *must be chosen to obey the condition:*

$$\beta > \max_{u,v}[V(u,v)+\rho_{u,v}U(u,v)].$$

Proof. The proof can be found in Itkin (2017a); Itkin (2017b).

The computational scheme in Equation (A5) should be understood in the following way. At the first line of Equation (A5) we begin with computing the product $\mathfrak{S}_1 = \alpha^+\overline{\mathfrak{S}}$. This can be done in three steps. First, the product $\mathfrak{S}_1 = Q\sqrt{\Delta T}\rho_{u,v}U(u,v)A^{1F}_{1,u}\overline{\mathfrak{S}}$ is computed in a loop on v_i, $i=1,\ldots,N_v$. In other words, if $\mathfrak{S}$ is a $N_u\times N_v$ matrix where the rows represent the u coordinate and the columns represent the v coordinate, each j-th column of $\mathfrak{S}_1$ is a product of matrix $Q\sqrt{\Delta T}\rho_{u,v}U(u,v)A^{1F}_{1,u}$ and the j-th column of $\overline{\mathfrak{S}}$. The second step is to compute the product $\mathfrak{S}_2 = P\sqrt{\Delta T}V(u,v)A^{1F}_{1,v}\overline{\mathfrak{S}}$, which can be done in a loop on u_i, $i=1,\ldots,N_u$. Finally, the right hand side of the first line in Equation (A5) is $(PQ+1)\overline{\mathfrak{S}}-\mathfrak{S}_1+\mathfrak{S}_2-\mathfrak{S}^j$. Then in a loop on u_i, $i=1,\ldots,N_u$, N_u systems of linear equations have to be solved, each giving a row vector of $\mathfrak{S}^*$. The advantage of the representation Equation (A5) is that the product $\alpha^+\overline{\mathfrak{S}}$ can be precomputed.

If $\sqrt{\Delta T}\approx\max(h_u,h_v)$, then the whole scheme becomes of the second order in space. However, this would be a serious restriction inherent to the explicit schemes. Therefore, we don't rely on it. Note, that in practice the time step is usually chosen such that $\sqrt{\Delta T}\ll 1$, and hence the whole scheme is expected to be closer to the second, rather than to the first order in h. Note, that this approach is similar to Toivanen (2010); Chiarella et al. (2008) for negative correlations, where a seven point stencil breaks a rigorous second order of approximation in space.

As shown in Itkin (2017a), the rate of convergence of the Picard iterations is linear.

The above results can be further improved by making the whole scheme be of the second order of approximation in h_u and h_v. We call this FD scheme as Scheme B.

Proposition A.2. *Let us approximate the left hand side of Equation (A4) using the following finite-difference scheme:*

$$\begin{aligned}&(QI_v+\sqrt{\Delta T}V(u,v)A^{2B}_{1,v})\mathfrak{S}^* = \alpha^+_2\overline{\mathfrak{S}}-\mathfrak{S}^j,\\&(PI_u-\sqrt{\Delta T}\rho_{u,v}U(u,v)A^{2B}_{1,u})\mathfrak{S}^{j+1} = \mathfrak{S}^*,\\&\alpha^+_2 = (PQ+1)I-Q\sqrt{\Delta T}\rho_{u,v}U(u,v)A^{2F}_{1,u}+P\sqrt{\Delta T}V(u,v)A^{2F}_{1,v}.\end{aligned} \tag{A6}$$

Then this scheme is unconditionally stable in time step $\mathbb{D}T$*, approximates Equation (A4)* with $O(\max(h_u^2,h_v^2))$ *and preserves positivity of the vector* $\mathfrak{S}(u,x,T)$ *if* $Q=\beta\sqrt{\Delta T}/h_v$, $P=\beta\sqrt{\Delta T}/h_u$*, where* h_v, h_u *are the grid space steps correspondingly in* v *and* u *directions, and the coefficient* β *must be chosen to obey the condition:*

$$\beta > \frac{3}{2}\max_{u,v}[V(u,v)+\rho_{u,v}U(u,v)].$$

The scheme Equation (A6) has a linear complexity in each direction.

Proof. See Itkin (2017a).

The coefficient β should be chosen experimentally. In our experiments described in the following sections, we used

$$\beta = \max_{u,v}[U(u,v)-\rho_{u,v}U(u,v)]. \tag{A7}$$

[7] The reader shouldn't miss these iterations (marked by j) used to solve Equation (A1) with those (marked by k) for the solution of the nonlinear equations, which are discussed towards the end of the article.

[8] For the sake of clarity, we formulate this Proposition for the uniform grid, but it is transparent how to extend it for the non-uniform grid.

APPENDIX B

NORM OF THE FRÈCHET DERIVATIVE FOR OPERATORS IN EQUATION (60)

To compute the norm of the Frèchet derivative, recall that by definition

$$\|\mathbb{D}(\varepsilon)\| = \sup_{\nu \neq 0} \frac{\|\mathbb{D}(\varepsilon)(\nu)\|}{\|\nu\|}$$

If $\nu = (\nu_1, ..., \nu_m) \in [L^{\infty}(-\infty, 0)]^m$, then

$$\mathbb{D}(\varepsilon)(\nu) = \left. \frac{\partial \varepsilon(\mathfrak{S} + k\nu)}{\partial k} \right|_{k=0}.$$

In other words, in this case the Frèchet derivative coincides with the Gâteaux derivative.

To find $\mathbb{D}(e^{NL})(\mathfrak{S})$, we need some results from functional analysis, namely:

1. The product and quotient rules for the Frèchet derivatives, Schwartz and Karcher (1969).
2. The property that the Frèchet derivative of a linear operator is the operator itself, Schwartz and Karcher (1969).
3. Let $A \rightarrow A^r$ be the map that takes a positive definite matrix to its r-th power, and let $\mathbb{D}A^r$ be the Frèchet derivative of this map. Then it is known that $||\mathbb{D}A^r|| = ||rA^{r-1}||$ if $r \leq 1$ or $r \geq 2$, Bhatia and Holbrook (2003).
4. Triangle inequality.

Let us denote the nonlinear part of $\tilde{\mathcal{L}}$ as $\tilde{\mathcal{L}}^{NL}$, and the linear part—as $\tilde{\mathcal{L}}^{L}$. Accordingly, $\tilde{\mathcal{L}} = \tilde{\mathcal{L}}^{NL} + \tilde{\mathcal{L}}^{L}$. Using the properties of the Frèchet derivatives, we obtain

$$\begin{aligned} \|\mathbb{D}(\Delta T L_u^{NL})(\mathfrak{S})\| &\leq \frac{\Delta T}{2T} \left\| \left(\frac{\mathfrak{S}_v[c_1(1-u)+a\nu]}{a\mathfrak{S}_u + c_1\mathfrak{S}_v} \right)^2 (2\mathfrak{S} + \mathfrak{S}^2)\nabla_u^2 \right\| \\ &\leq \frac{\Delta T}{2T} \left\| \frac{\mathfrak{S}_v[c_1(1-u)+a\nu]}{a\mathfrak{S}_u + c_1\mathfrak{S}_v} \right\|^2 \|\mathfrak{S}(2+\mathfrak{S})\| \|\nabla_u^2\|. \end{aligned} \tag{B1}$$

It can be seen that the first norm $||\cdot||_1$ in the right hands part of Equation (B1) is bounded, and moreover, $||\cdot||_1 \leqslant 2$. The second norm $||\cdot||_2$ is also bounded since we work on a truncated grid with $K < K_{\max}$. Therefore, the values of $\mathfrak{S}$ are also bounded. For instance, in our numerical experiments $\mathfrak{S} < 8$. For the third norm $\left\|\nabla_u^2\right\|$, it is well-known, Starzak (1989), that at the uniform grid

$$\|\nabla_u^2\| = \max_i \left[\frac{4}{h_u^2} \sin^2 \frac{i\pi}{2(N_u+1)} \right], \quad i \in [1, ..., N_u], \tag{B2}$$

where N_u is the size of the matrix $A_{2,u}^C$, and h_u is the grid step. For the uniform grid $h_u = 1/(N_u - 1)$. Therefore,

$$\left\| \mathbb{D}(\Delta T L_u^{NL})(\mathfrak{S}) \right\| \leq 2\, \Delta T \frac{2}{h_u^2} \|\Sigma\|^2 \tag{B3}$$

where $\|\Sigma\|$ is the norm of matrix $A(\Sigma)$ on the grid.

A similar analysis can be provided for the norm $\left\|\mathbb{D}(\Delta T L_v^{NL})(\mathfrak{S})\right\|$ to obtain

$$\left\| \mathbb{D}(\Delta T L_u^{NL})(\mathfrak{S}) \right\| \leq 2\, \Delta T \frac{1}{h_v^2} \|\Sigma\|^2 \tag{B4}$$

since

$$\left\| \frac{\mathfrak{S}_u[c_1(1-u)+a\nu]}{a\,\mathfrak{S}_u + c_1\,\mathfrak{S}_v} \right\|^2 \leq 1.$$

Finally, for the mixed derivative term, we have

$$\begin{aligned} &\left\| \mathbb{D}(-\Delta T L_{uv}^{NL})(\mathfrak{S}) \right\| \\ &\quad \leq \frac{\Delta T}{T} \left\| \left(\frac{c_1(1-u)+a\nu}{a\mathfrak{S}_u + c_1\mathfrak{S}_v} \right)^2 \mathfrak{S}_u\mathfrak{S}_v\nabla_{uv}(2\mathfrak{S} + \mathfrak{S}^2) \right\|. \end{aligned} \tag{B5}$$

Similarly to Equation (B2),

$$\begin{aligned} \left\| \nabla_u \nabla_v \right\| &= \max_{i,j} \left[\frac{4}{h_u h_v} \sin \frac{i\pi}{2(N_u+1)} \sin \frac{j\pi}{2(N_v+1)} \right], \\ &i \in [1, ..., N_u],\ j \in [1, ..., N_v], \end{aligned} \tag{B6}$$

and also

$$\left\| \left(\frac{c_1(1-u)+a\nu}{a\mathfrak{S}_u + c_1\mathfrak{S}_v} \right)^2 \mathfrak{S}_u\ \mathfrak{S}_v \right\| \leq \frac{3}{2}.$$

Therefore,

$$\left\| \mathbb{D}(\Delta T L_{uv}^{NL})(\mathfrak{S}) \right\| \leq 2\Delta T \frac{3}{h_v h_u} |\Sigma|^2. \tag{B7}$$

Finally, using these expressions, and properties of the Frèchet derivatives, we obtain

$$\|\mathbb{D}(\varepsilon)(\mathfrak{S})\| = \Delta T \|\varepsilon\| \left\| \mathbb{D}\left(\frac{\partial \varepsilon}{\partial \Delta T}\right)(\mathfrak{S}) \right\|$$
$$\le \Delta T \|\varepsilon\| \left(||\Sigma||^2 \left| \frac{1}{h_u^2} + \frac{2}{h_u^2} - \frac{3}{h_v h_u} \right| + \|L^L\| \right), \tag{B8}$$

where $||L^L||$ is the norm of the linear part of the operator $\tilde{\mathcal{L}}_u^{(k-1)} + \tilde{\mathcal{L}}_v^{(k-1)} + \tilde{\mathcal{L}}_{uv}^{(k-1)}$ in Equation (60). It is easy to show that

$$\left\| L^L \right\| \le \alpha^L \left| \frac{1}{h_u} + \frac{1}{h_v} \right|,$$

where $|\alpha^L| \le 1$.

As we mentioned already, on the FD grid $||\varepsilon||$ is a spectral norm of the matrix exponential e^{M}, where

$$\left\| \mathcal{M} \right\| \le \Delta T \left(\alpha^{NL} ||\Sigma||^2 \left| \frac{1}{h_u^2} + \frac{2}{h_u^2} - \frac{3}{h_v h_u} \right| + \alpha L \left| \frac{1}{h_u} + \frac{1}{h_v} \right| \right).$$

Here α^{NL}, α^L are some terms that don't depend on ΔT, h_u, h_v, i.e., on the FD steps in all spatial and temporal directions. Also, by construction $M = A(\mathcal{M})$ is the Metzler matrix with all eigenvalues being negative. Therefore, it can be seen that by decreasing the steps h_u, h_v, or increasing the step ΔT, we decrease the norm $||\mathbb{D}(\varepsilon)(\mathfrak{S})||$ (as the exponential term dominates). Therefore, to decrease the norm $||\mathbb{D}(\varepsilon)(\mathfrak{S})||$ we can, e.g., fix the time step DT, and then decrease the step h_u or h_v (or both) until we get $||\mathbb{D}(\varepsilon)(\mathfrak{S})|| < 1$.

This could be compared with the familiar stability condition for the Euler explicit FD scheme, which reads, Itkin (2017b)

$$2D \frac{\Delta T}{h^2} \le 1, \tag{B9}$$

with D being some diffusion coefficient. The latter condition is restrictive, because it sets the upper limit on the time step, given the space step h. In contrast, our condition, using a loose notation, reads

$$2D \frac{\Delta T}{h^2} > 1.$$

Since this is a stability condition, the convergence of our iterative method is conditional. However, our condition is far less restrictive than that in Equation (B9). Indeed, given the space step h, we need the time step to *exceed* the value $h^2/(2D)$, while Equation (B9) requires it to be *less* than $h^2/(2D)$. Since h^2 is normally small, and D is proportional to $||\Sigma||^2 > 1$ on the grid, it could be satisfied with no serious restrictions on ΔT. Therefore, the iterative scheme is "almost" unconditionally stable, where "almost" means - at the values of the model parameters that are reasonable from a practical point of view.

ACKNOWLEDGMENTS

We thank Archil Gulisashvili and Daniel Duffy for useful discussions, and an anonymous referee for some helpful comments. Any errors are our own.

REFERENCES

Benaim, S., and P. Friz. 2009. "Regular Variations and Smile Asymptotics." *Mathematical Finance* 19: 1–12.

Berman, A., and R. Plemmons. 1994. *Nonnegative Matrices in Mathematical Sciences*. SIAM.

Bhatia, R., and J. A. Holbrook. 2003. "Frechet Derivatives of the Power Function." *Indiana Univ. Math. Journal* 49: 1155–1173.

Chiarella, C., et al. 2008. *The Evaluation of American Option Prices Under Stochastic Volatility and Jump-Diffusion Dynamics Using the Method of Lines*. Tech. Rep. Research paper 219, Quantitative Finance Research Centre, University of Technology, Sydney.

Corcuera, J. M., et al. 2009. "Implied Lévy Volatility." *Quantitative Finance* 9 (4): 383–393.

Craig, I. J. D., and A. D. Sneyd. 1988. "An Alternating-Direction Implicit Scheme for Parabolic Equations with Mixed Derivatives." *Comp. Math. Appl.* 16: 341–350.

Dawidowski, Ł. 2017. "The Quasilinear Parabolic Kirchhoff Equation." *Open Mathematics* 15 (1): 382–392.

Douglas, Jr., J., and H. H. Rachford, Jr. 1956. "On the Numerical Solution of Heat Conduction Problems in Two and Three Space Variables." *Transactions of the American Mathematical Society* 82: 421–439.

Duffy, D. J. 2006. *Finite Difference Methods in Financial Engineering: A Partial Differential Equation Approach*. The Wiley Finance Series.

Dupire, B. 1994. "Pricing with a Smile." *Risk* 7: 18–20.

Dyakonov, E. G. 1964. "Difference Schemes with a Separable Operator for General Second Order Parabolic Equations with Variable Coefficient." *Zhurnal Vychislitelnoi Matematiki i Matematicheskoi Fiziki* 4 (2): 278–291.

Gasull, A., and F. Utzet. 2013. "Approximating Mills Ratio." July. Available at http://arxiv.org/pdf/1307.3433v1.pdf.

Gatheral, J. 2006. *The Volatility Surface*. Wiley Finance, 179.

Glau, K., et al. 2018. "The Chebyshev Method for the Implied Volatility." *Journal of Computational Finance*. Forthcoming.

Glowinski, R., T. W. Pan, and X. C. Tai. 2016. "Some Facts about Operator-Splitting and Alternating Direction Methods." *Splitting Methods in Communication, Imaging, Science, and Engineering*. Ed. by R. Glowinski, S. J. Osher, and W. Yin. Springer International Publishing. Chap. 2. ISBN: 978-3-319-41587-1.

Gobbino, M. 1999. "Quasilinear Degenerate Parabolic Equations of Kirchhoff Type." *Math. Meth. Appl. Sci*. 22: 375–388.

Granas, A., and J. Dugundji. 2003. *Fixed Point Theory*. New York: Springer-Verlag.

Gulisashvili, A. 2010. "Asymptotic Formulas with Error Estimates for Call Pricing Functions and the Implied Volatility at Extreme Strikes." *Siam J. Financial Math* 1: 609–641.

Haentjens, T., and K. J. In't Hout. 2012. "Alternating Direction Implicit Finite Difference Schemes for the Heston–Hull–White Partial Differential Equation." *Journal of Computational Finance* 16: 83–110.

Hochschild, G. P. 1981. *Basic Theory of Algebraic Groups and Lie Algebras*. Graduate Texts in Mathematics. Springer-Verlag. ISBN: 9783540905417.

Hull, J. C. 1997. *Options, Futures, and Other Derivative Securities*. Third edition. Upper Saddle River, NJ: Prentice-Hall, Inc.

Hutson, V., J. Pym, and M. Cloud. 2005. *Applications of Functional Analysis and Operator Theory*. Mathematics in Science and Engineering. Elsevier Science. ISBN: 9780080527314.

In't Hout, K. J., and S. Foulon. 2010. "ADI Finite Difference Schemes for Option Pricing in the Heston Model with Correlation." *International Journal of Numerical Analysis and Modeling* 7 (2): 303–320.

In't Hout, K. J., and B. D. Welfert. 2007. "Stability of ADI Schemes Applied to Convection-Diffusion Equations with Mixed Derivative Terms." *Applied Numerical Mathematics* 57: 19–35.

Itkin, A. 2016. "Efficient Solution of Backward Jump-Diffusion Partial Integro-Differential Equations with Splitting and Matrix Exponentials." *J. Comput. Financ*. 19 (3): 29–70.

—— 2017a. "LSV Models with Stochastic Interest Rates and Correlated Jumps." *International Journal of Computer Mathematics* 94 (7): 1291–1317.

—— 2017b. *Pricing Derivatives under Lévy Models. Modern Finite-Difference and Pseudo-Differential Operators Approach*. Vol. 12 Pseudo-Differential Operators. Birkhauser.

—— 2018. "Nonlinear PDEs Risen when Solving Some Optimization Problems in Finance, and their Solutions." *Journal of Computational Finance* 21 (4): 1–21.

—— 2019. "Deep Learning Calibration of Option Pricing Models: Some Pitfalls and Solutions." Arxiv: 1906.03507. url: https://arxiv.org/abs/1906.03507.

Itkin, A., and P. Carr. 2011. "Jumps without Tears: A New Splitting Technology for Barrier Options." *International Journal of Numerical Analysis and Modeling* 8 (4): 667–704.

Jackel, P. 2015. "Let's Be Rational." *Wilmott Magazine* 75: 40–43.

Katsumi, N., and S. Sasaki. 1994. *Affine Differential Geometry*. Cambridge University Press. ISBN: 978-0-521-44177-3.

Kirchhoff, G. 1883. *Vorlesungen über Mechanik*. Stuttgart: Teubner.

Lanser, D., and J. G. Verwer. 1999. "Analysis of Operator Splitting for Advection-Diffusion-Reaction Problems from Air Pollution Modelling." *Journal of Computational and Applied Mathematics* 111 (1–2): 201–216.

Lee, R. 2004. "The Moment Formula for Implied Volatility at Extreme Strikes." *Mathematical Finance* 14 (3): 469–480.

Li, B., et al. 2010. "Solutions to a Reduced Poisson-Nernst-Planck System and Determination of Reaction Rates." *Physica A* 389: 1329–1345.

Lucic, V. 2008. *Boundary Conditions for Computing Densities in Hybrid Models via PDE Methods*. July. SSRN 1191962.

Nakao, M. 2009. "An Attractor for a Nonlinear Dissipative Wave Equation of Kirchhoff Type." *J. Math. Anal. Appl*. 353: 652–659.

Natenberg, S. 1994. *Option Volatility & Pricing: Advanced Trading Strategies and Techniques*. McGraw-Hill Education. ISBN: 9781557384867.

Nikol'skii, S. M. 1953. "The Properties of Certain Classes of Functions of Many Variables on Differentiable Manifolds." *Mat. Sb.* (*N.S.*) 33 (75) 2: 261–326. URL: http://www.mathnet.ru/links/b2f634e1d228d8afd8cde7d719e240fe/sm5351.pdf.

Oleinik, O. A., and E. V. Radkevich. 1973. *Second Order Equations with Non-Negative Characteristic Form*. Kluwer Academic Publishers.

Peaceman, D. W., and H. H. Rachford, Jr. 1955. "The Numerical Solution of Parabolic and Elliptic Differential Equations." *Journal of Society for Industrial and Applied Mathematics* 3: 28–41.

Pealat, G., and D. J. Duffy. 2011. "The Alternating Direction Explicit (ADE) Method for One Factor Problems." *Wilmott Magazine* 9.

Pinchover, Y., and J. Rubinstein. 2005. *An Introduction to Partial Differential Equations*. Cambridge University Press. ISBN: 9780511110252.

Roach, P. J. 1976. *Computational Fluid Dynamics*. Hermosa Publishers.

Samarski, A. 1964. "Economical Difference Schemes for Parabolic Equations with Mixed Derivatives." *Zhurnal Vychislitelnoi Matematiki i Matematicheskoi Fiziki* 4 (4): 753–759.

Saul'yev, V. K. 1964. *Integration of Equations of Parabolic Type by the Method of Nets*. Ed. by I. N. Sneddon, M. Stark, and S. Ulam. Oxford: Pergamon Press. ISBN: 9781483155326.

Schwartz, J. T., and H. Karcher. 1969. *Nonlinear Functional Analysis*: *Notes on Mathematics and its Applications*. Gordon & Breach.

Starzak, M. E. 1989. *Mathematical Methods in Chemistry and Physics*. New York: Springer.

Strang, G. 1968. "On the Construction and Comparison of Difference Schemes." *SIAM J. Numerical Analysis* 5: 509–517.

Toivanen, J. 2010. "A Component-Wise Splitting Method for Pricing American Options under the Bates Model." *Computational Methods in Applied Sciences* Springer, 213–227.

Wahbi, I. 2018. "Quasi Linear Parabolic PDE in a Junction with Nonlinear Neumann Vertex Condition." *Journal of Mathematical Analysis and Applications*. URL: https://hal.archives-ouvertes.fr/hal-01833719.

Yanenko, N. 1971. *The Method of Fractional Steps*. Springer-Verlag.

ADDITIONAL READING

Geometric Local Variance Gamma Model

P. Carr and A. Itkin
The Journal of Derivatives
https://jod.pm-research.com/content/27/2/7

ABSTRACT: *This article describes another extension of the local variance gamma model originally proposed by Carr in 2008 and then further elaborated by Carr and Nadtochiy in 2017 and Carr and Itkin in 2018. As compared with the latest version of the model developed by Carr and Itkin and called the "expanded local variance gamma" (ELVG) model, two innovations are provided in this article. First, in all previous articles the model was constructed on the basis of a gamma time-changed arithmetic Brownian motion: with no drift in Carr and Nadtochiy, with drift in Carr and Itkin, and with the local variance a function of the spot level only. In contrast, this article develops a geometric version of this model with drift. Second, in Carr and Nadtochiy the model was calibrated to option smiles assuming that the local variance is a piecewise constant function of strike, while in Carr and Itkin the local variance was assumed to be a piecewise linear function of strike. In this article, the authors consider three piecewise linear models: the local variance as a function of strike, the local variance as a function of log-strike, and the local volatility as a function of strike (so, the local variance is a piecewise quadratic function of strike). The authors show that for all these new constructions, it is still possible to derive an ordinary differential equation for the option price, which plays the role of Dupire's equation for the standard local volatility model, and moreover, it can be solved in closed form. Finally, similar to in Carr and Itkin, the authors show that given multiple smiles the whole local variance/volatility surface can be recovered without requiring solving any optimization problem. Instead, it can be done term-by-term by solving a system of nonlinear algebraic equations for each maturity, which is a significantly faster process.*

Constructing Equity Portfolios from SEC 13F Data Using Feature Extraction and Machine Learning

Alexander Fleiss, Han Cui, Sasha Stoikov, and Daniel M. DiPietro

The Journal of Financial Data Science
https://jfds.pm-research.com/content/2/1/45

ABSTRACT: *Securities and Exchange Commission (SEC) form 13F allows the public a quarterly glimpse of the holdings of top asset managers. Here the authors propose two novel quantitative approaches for constructing portfolio-generating models based on these data, as well as guidelines for feature extraction. The first examined approach uses extracted features from 13F data to predict stock price movements. Stocks that are predicted to have positive returns are then used to assemble a portfolio. The second approach uses extracted features to identify top funds and then assembles their holdings into an aggregate portfolio. Both techniques outperformed the S&P 500 in historical backtesting, earning an annualized 15.0% and 19.8%, respectively, compared with 9.5% for the S&P 500. Overall, these results build on additional statistical approaches for creating quantitative models with SEC 13F data, in addition to offering a previously unexplored machine learning approach that outperforms the benchmark.*

QUERIES

AQ1
Page 1
Please provide complete mailing addresses, phone numbers, and e-mail addresses for all authors on the article. Failure to do so will result in authors not receiving their complimentary print copies.

AQ2
Page 8
Please provide editable source file or high resolution image for Exhibit 2.